

# Credit risk — a structural model with jumps and correlations

Rudi Schäfer,<sup>\*</sup> Markus Sjölin, Andreas Sundin, Michal Wolanski, and Thomas Guhr<sup>†</sup>

*Department of Mathematical Physics, LTH, Lund University, Sweden*

(Dated: December 2, 2008)

We set up a structural model to study credit risk for a portfolio containing several or many credit contracts. The model is based on a jump–diffusion process for the risk factors, i.e. for the company assets. We also include correlations between the companies. We discuss that models of this type have much in common with other problems in statistical physics and in the theory of complex systems. We study a simplified version of our model analytically. Furthermore, we perform extensive numerical simulations for the full model. The observables are the loss distribution of the credit portfolio, its moments and other quantities derived thereof. We compile detailed information about the parameter dependence of these observables. In the course of setting up and analyzing our model, we also give a review of credit risk modeling for a physics audience.

PACS numbers: 89.65.Gh, 05.40.Jc, 05.90.+m

Keywords: credit risk, econophysics, stochastic processes

## I. INTRODUCTION

Economics attracts the interest of a quickly growing community in physics. A large part of the research addresses the financial markets. Attempts are being made to better understand various phenomena such as the fat tails of the stock price distributions by relating them to physics systems, see Refs. [1, 2, 3] and references therein. Physicists have also joined the activities of economists and computer scientists in agent–based models [4, 5], and applied their long–standing experience in complex systems, see Ref. [6].

As far as the field of finance is concerned, the vast majority of studies put forward by physicists has been devoted to market risk. The market risk is due to the unknown time evolution of the asset prices. In general, one is faced with a large spectrum of different risk types. One also distinguishes, for example, operational risk (due to failure of internal systems), political risk (due to political decisions that affect the capital markets) and legal risk (due to fraud and discontinued contracts). In this contribution, we address credit risk. It is due to the failure of a counterpart to make a promised payment. At present, risk managers and researchers are more familiar with market risk than with any of the other risk types and the corresponding mathematical description is highly developed. It is of considerable practical interest to improve the knowledge about and the modeling of the other risk types. In the case of credit risk, the probability that a promised payment is not made is usually small and difficult to estimate. Nevertheless the amount of money involved and thus the associated loss can be enormous and even jeopardize the existence of the financial institution which issued the credit.

Only recently, physicists started applying their spe-

cific tools to credit risk [7, 8, 9, 10, 11, 12]. The interesting point for practitioners and researchers, especially statistical physicists, is the highly asymmetric form of the loss distribution and the resulting peculiar features. This distinguishes credit risk from market risk, although the former clearly depends on the latter. In investment theory the standard deviation, referred to as volatility, of the relative asset price change is taken as a measure of how risky a certain investment is. If more uncertainty is incorporated in the investment, i.e. if the volatility is larger, then the demanded earnings are higher. Due to this fact, investors are traditionally risk averse. In other words, a potential loss is considered to be more punitive than a potential gain is beneficial, even if they are equally probable and large. The asymmetric character of the loss distributions makes risk measures other than the volatility also important in credit risk management.

In this study, we set up and analyze a structural model for credit risk, based on a jump–diffusion process for the risk factors. Our study is related to, but different from the work in Ref. [13]. These models are particularly appealing to physicists, because their starting point is, in physics terminology, microscopic and dynamical. This gives them a rather general character which makes them also suited for other problems in physics and in the theory of complex systems. With this contribution, we pursue two goals. First, we systematically explore the interplay between the different parameters of our structural model, particularly the role of leverage, jumps and correlations. In contrast to the existing literature, our main focus is on the full loss distribution of the credit portfolio, its moments and its tail behavior. Second, we review credit risk modeling and keep the whole presentation pedagogical, because we want to make this topic more accessible to the physics audience.

The paper is organized as follows. We review the present status of credit risk modeling in Sec. II. In Sec. III we introduce our model. We discuss a simplified version of it analytically in Sec. IV and the full model numerically in Sec. V. Summary and conclusion are given in

<sup>\*</sup>Rudi.Schaefer@matfys.lth.se

<sup>†</sup>Thomas.Guhr@matfys.lth.se

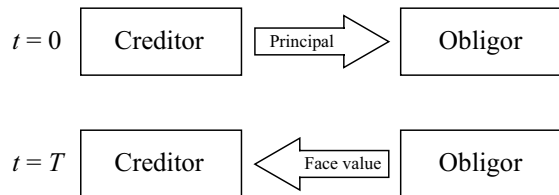


FIG. 1: The cash flow of a zero-coupon bond.

Sec. VI.

## II. CREDIT RISK MODELING

After defining debt instruments in Sec. II A, we discuss what one means by default and credit ratings in Secs. II B and II C, respectively. The credit risk measures are introduced in Sec. II D. The impact of correlations is discussed in Sec. II E. The rôle of the probability density function for credit losses is explained in Sec. II F. We conclude this short review by presenting the most important credit risk models in Sec. II G. Reviews in the financial literature on credit risk modeling can be found in Refs. [14, 15]

### A. Debt instruments

A debt instrument is simply a written promise to repay a debt. There is a wide range of such contracts. A debt instrument has two positions: a lending side (the creditor) and a borrowing side (the obligor). Bonds are very common. A bond is issued for a period of one year or more with the purpose of raising capital by borrowing. The government, states, cities, corporations, and many other types of institutions can sell bonds. Generally, a bond is a promise to repay the principal along with interest (coupons) on a specified date (maturity). The principal is the amount borrowed or the part of the amount borrowed which remains unpaid (excluding interest). Some bonds do not pay interest. In this study we focus on the *zero-coupon bond*. The cash flow of the zero-coupon bond is limited to two dates: the date of issue  $t = 0$  and maturity  $t = T$ . At the issue date the creditor lends a specified amount of money to the obligor. At maturity, the obligor has to repay the face value of the bond. The face value is the amount borrowed plus interest and additional yield compensating for the risk. Fig. 1 shows the cash flow of the zero-coupon bond.

### B. Default event

The key issue which separates credit risk from, for example, market risk, is the concept of default. Its definition is not homogeneous throughout the industry of credit risk management. Usually default means that

there has been a missed or delayed payment of interest and/or principal within a grace period, or that an obligor files for bankruptcy [16]. Although default is a truly rare event, creditors can lose large amounts of money. A good example is the bankruptcy of *Enron Corporation* in Dec. 2, 2001. At an asset value of US \$49.53 billion, this was the largest bankruptcy filing in US history to that date [17]. The actual loss for the creditors was US \$9.9 billion [16].

### C. Credit ratings

A way to quantify credit risk is to determine the credit worthiness of a potential customer from the historical performance of the obligors. There is a wide range of rating systems for credit worthiness, systems used internally by the credit institute as well as external ratings available for public. The credit rating of a company is often directly linked to the probability that the company defaults within a fixed time horizon, usually one year. Two frequently used rating systems are Standard & Poor's and Moody's. The probability that a company changes its credit rating is expressed in terms of a rating transition matrix which contains the probabilities that a company with a certain rating migrates to another category, usually within a year. The credit rating transition matrix is based on the historical migration frequencies of corporate bonds. It is observed that the most probable future event is that the company remains in the same rating category. This is valid for all rating categories. Moreover, the probability of a downgrade is generally higher than the probability of an upgrade [18].

### D. Credit risk observables

There are several ways of quantifying credit risk. We distinguish between standalone risk and portfolio risk [19]. The most frequently used standalone observables are the default probability (DP), the loss given default (LGD) and the migration risk. The conventional portfolio risk observables are default correlations and exposure, i.e. the size, or proportion, of a credit portfolio exposed to default risk.

### E. Correlations

The credit worthiness of obligors often involves mutual correlations. For example, defaults are more frequent in times of regression in the surrounding economy. Furthermore, one can see that companies in the same country and/or industry can affect each others rating migrations, up as well as down [14]. There are different ways to incorporate correlations between default events of obligors. For example, one uses the correlations between the equity values of the companies, i.e. the stocks, to describe

the dependency of credit migrations. Another way to examine this is to look at how the obligors depend on the current state of the economy [20]. Modeling correlations is often difficult because only limited data are available for the indicators chosen. Moreover, because of the huge number of correlations involved in a normal sized credit portfolio (which can contain a few thousand bonds), it is necessary to make simplified assumptions. A common procedure is to categorize the companies into different groups or branches with specified correlations. For example, one can assume correlations which are country-specific, industry-specific etc. Even though these simplifications lead to a more manageable model, it is still a complicated task to decide the structure of the categorization and to estimate the group-specific correlations.

### F. Probability density function of credit losses

The primary output of a credit risk model is the probability density function (PDF) of credit losses for a given portfolio. Adapting to the more common physics terminology, we refer to this function as the loss *distribution*. Here we make the assumption that the loss is a continuous random variable, so that we can work directly with the PDF. From the loss distribution one determines the expected loss EL, the unexpected loss UL, the required risk capital and further quantities. The expected loss EL is the mean of the loss distribution and the unexpected loss UL is its standard deviation. It is important to notice that UL, not EL, measures risk. However, to cover potential losses it is not enough to have a “cushion” within the standard deviation. The probability that losses exceed the UL is significant and it is therefore necessary to have another measure of risk capital. To quantify risk capital one usually uses the economic capital EC which is also known as Capital at Risk CaR or as the Value at Risk VaR. The economic capital EC is defined as the difference between the expected loss EL and the  $\alpha$ -quantile for a certain level of confidence. Figure 2 shows a typical loss distribution with EL, UL and EC. The general appearance of such a loss distribution is different from the distributions in, for example, market risk. While the distributions of market risk are typically Gaussian, the distributions generated by credit risk are *skewed* and *leptokurtic* [14].

To measure the important tail behavior, one uses the kurtosis excess. We recall that the kurtosis  $\beta_2$  is defined as the fourth central moment divided by the squared second central moment. The kurtosis excess  $\gamma_2$  is the part of the kurtosis that exceeds the kurtosis of the normal distribution (which is equal to 3), i.e.  $\gamma_2 = \beta_2 - 3$ . A distribution is often referred to as fat-tailed if it is leptokurtic, i.e.  $\gamma_2 > 0$ . Fat-tailed distributions have higher quantiles than a normal distribution and thus require more attention from a credit risk manager.

To generate a loss distribution of a credit portfolio, one can evaluate it for a structural model either analytically

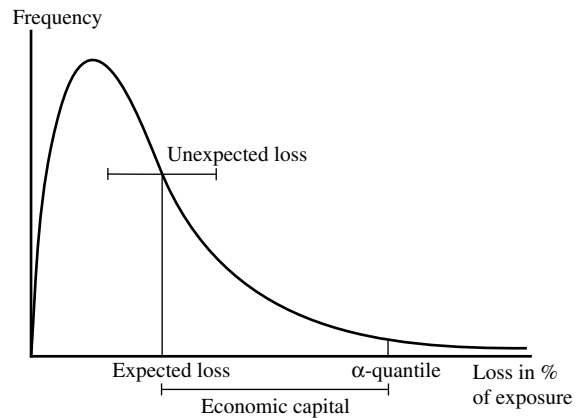


FIG. 2: A schematic loss distribution with the expected loss EL, the unexpected loss UL and the economic capital EC.

(in some simple cases) or numerically by Monte Carlo simulation. It is also possible to approximate an actual portfolio distribution by some known analytical distribution. In the latter case, one maps the actual portfolio with unknown distribution to an equivalent portfolio with a known distribution. A frequently used distribution which has the right features, i.e. skewed and fat-tailed, is the beta distribution [14]. A better and more sophisticated approach than parametric approximations is offered by reduced form models. Some of these models lead to analytically tractable loss distributions, see e.g. Ref. [21] and references therein.

### G. Credit risk models

Current credit risk models can be divided into two main categories: structural models and reduced form models.

In the *structural models* one makes assumptions about the time evolution of the risk factors, i.e. mostly the asset or stock prices of the companies, as well as about the liabilities. Whenever the asset value falls below some specified threshold, like the book value of the liabilities, the firm defaults. The structural credit risk modeling approach has its roots in the Black and Scholes theory for option pricing, and the Merton model, see Ref. [14]. The Black and Scholes theory is based on the assumption of a friction-less market where the stock or asset price is described by a geometric Brownian motion. Merton viewed the equity value of a company as a call option of the asset value with a strike price equal to the face value  $F$  of the debts. It is assumed that the company has a certain amount of zero-coupon debt due at a future time  $T$ . In consequence, it is possible to apply the whole Black and Scholes machinery to the credit risk modeling problem [14]. This is the “microscopic” viewpoint which makes structural models suitable for physics approaches.

The *reduced form models* for credit risk are based on

the assumption of a functional relationship between the obligors' expected default rates and different background factors. These background factors may represent either observable or unobservable variables. Observable variables typically depend on the general state of the economy, and the unobservable variables often represent some random risk factors [20]. The event of default is often modeled by an intensity process, e.g. a Poisson process. Unlike the structural approach, the reduced form approach is not directly based on a dynamical description of the economy. Reduced form models are often implemented as black-box models, where the accuracy of the model outcome is more important than an intuitive economical interpretation of the mechanisms included in the black box.

One of the key issues when setting up a credit risk model is to define an event that leads to an actual loss. Usually, credit risk modelers use either of two definitions of credit loss: the default mode paradigm, or the mark-to-market paradigm. Within the *default mode* (DM) paradigm, a credit loss occurs only when an obligor defaults within the bonds maturity time. Within the *mark-to-market* (MTM) paradigm a credit loss can occur without an actual default. The creditor can lose money whenever an obligor's credit worthiness deteriorates. Both of these two modeling approaches are common in current vendor credit risk frameworks. Typical arguments for using one of them are the simplicity of the DM model and the multi-state nature of the MTM model. The DM model suits better for creditors which only are interested in a buy-and-hold portfolio, while the MTM model is more adequate for pricing decisions of more liquid credits [20].

There is a wide range of different credit risk management tools available in the financial industry. Many of those models seek to estimate the full distribution to be able to calculate different statistics measures [20]. Examples of vendor credit risk models are CreditMetrics (by RiskMetrics Group), PortfolioManager (by KMV), CreditPortfolioView (by McKinsey & Co), and CreditRisk<sup>+</sup> (by Credit Suisse Financial Products), see Ref. [22] and a review in Ref. [23].

### III. A MODEL WITH JUMPS AND CORRELATIONS

We set up our structural credit risk model in Sec. III A. In Sec. III B, we discuss its generality by relating it to a few other scenarios where structural models can find application.

#### A. Setup of the model

We model the time evolution of the asset value of every company by a stochastic differential equation of the form

$$\frac{dV}{V} = \mu dt + \sigma \varepsilon \sqrt{dt} + dJ . \quad (1)$$

Apart from the jump term  $dJ$ , this is a geometric Brownian motion with a deterministic term  $\mu dt$  describing the exponential growth of the asset value and a stochastic term  $dW = \varepsilon \sqrt{dt}$  representing the fluctuations as a Wiener process. Here,  $\mu$  is the drift,  $\sigma$  the volatility (constant) and  $\varepsilon$  an independently distributed random number in each time step. We add the jump term  $dJ$  which is not contained in Merton's original model. In previous works, jump-diffusion models have been considered for stock returns (see e.g. Ref. [24]) and also for credit risk [13, 25, 26, 27]. The economical interpretation of the jump term is that a major setback of an asset value is possible at any time. These setbacks are larger than the volatility admits and may be explained by events labeled as crises, originating from legal, operational, political or other external or internal factors. The probability that an economical setback takes place during the lifetime of a bond is typically very small. Well known examples of such economical setbacks for a large group of companies are the great stock market crash of 1929, the oil crisis of the mid-seventies and the "Black Monday" crash in 1987. We model the jumps by a *Poisson process* with intensity  $\lambda$ . We recall that, in such a process, the probability function for the event to occur  $n$  times between zero and the time  $t$  is given by

$$p_n^{\text{Poisson}}(t) = \frac{(\lambda t)^n}{n!} \exp(-\lambda t) . \quad (2)$$

The size  $\Lambda$  of the jump, measured in units of the current asset value  $V(t)$ , is a random variable with a distribution which we have to specify. Jumps can be positive or negative. The largest possible negative jump is 100% of the current asset value. Based on this information, a possible distribution of the jump size  $\Lambda$  is a shifted lognormal distribution,  $\Lambda + 1 \sim \text{LN}(\mu_J + 1, \sigma_J)$ , with mean  $\mu_J$  and standard deviation  $\sigma_J$ . A time series for the asset value including a negative jump is shown in Fig. 3. Without the jump term, the distribution of the asset price  $V(t)$  is log-normal. The jumps render the tails of the asset price distribution fatter. Fat tails are empirically observed [1]. As this clearly affects the loss distribution, we find it important to include such jumps. The parameters of the jump process can be adjusted in order to match the tail behavior of a given empirical time series of the asset value.

To determine if default has occurred, we compare the asset value at maturity  $T$  to the company's financial obligations, i.e. the face value  $F$  of the bond. This is in distinction to the so-called first-passage models, see e.g. Refs. [13, 25, 28], where default occurs as soon as

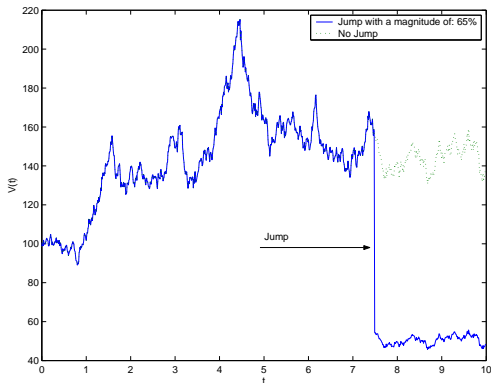


FIG. 3: Two time series for the asset value  $V(t)$  versus time  $t$ . They are equivalent except that one of them includes a large negative jump given by the jump term  $J(t)$ . The lower time series is damped because the factor  $V$  in Eq. (1) is much smaller after the jump.

the asset value  $V(t)$ , with  $0 \leq t \leq T$ , falls below some specified threshold function  $D(t)$ . For simplicity, we do not choose such a function and work with the face value  $F$ . In Fig. 4, the asset value process with the threshold is visualized. We employ the default mode paradigm, which means that an actual loss only occurs in case of a default. The size of the loss in case of default is given by the face value of the loan minus the total asset value at maturity. We normalize the loss to the face value  $F$ ,

$$L = \frac{F - V(T)}{F}, \quad (3)$$

implying that we have  $0 \leq L \leq 1$  for the normalized loss  $L$ . Many studies assume, for the sake of simplicity, that everything is lost in case of default, i.e.  $L$  can only take the values 0 and 1, see e.g. Refs. [28, 29]. In this simple case, many distinctive features of the loss distribution, as seen e.g. in Fig. 12, cannot be reproduced, and, particularly, the tail behavior of the loss distribution is different. Zhou [13] studied a first-passage model for credit risk based on a jump-diffusion process. This leads to a recovery rate which depends solely on the jump process, whereas in our model it is  $V(T)/F$ , i.e. it is determined by the whole asset process. In Ref. [13] default probability and credit spread are studied in dependence of maturity  $T$ . The present study is different, because we we extensively examine the full loss distribution of the credit portfolio.

It is important to include correlations between the companies in our model. We mention that financial correlations presently find considerable interest in the econophysics community. These correlations are noise dressed if measured for finite time series. The impact of noise dressing on portfolio optimization and methods how to reduce the noise to find the true correlations are much discussed in the literature [30, 31, 32, 33, 34, 35, 36, 37, 38]. The influence of noise dressing on credit risk has very recently been studied in Ref. [7]. To model the cor-

relations, we employ Noh's model [39] which belongs to the class of factor and arbitrage pricing models [28, 40]. Noh's model produces correlated normalized time series  $M_k(t)$ . We use the conventions of Ref. [38].

To achieve realistic portfolio correlations we divide the companies into different branches  $b = 1, 2, \dots, B$ . The total number of branches represented in a portfolio is given by the number  $B$ . The different companies in the portfolio are given by the index  $k = 1, 2, \dots, K$  and the branch index  $b$  is a function of the company index, i.e.  $b = b(k)$ . The number of companies in a specific branch  $b$  is given by  $\kappa_b$ . For the companies that are in no branch we have  $b = 0$ , and the number of those companies is given by  $\kappa$ . This means that we can write the total number of obligors  $K$  in a portfolio as

$$K = \kappa + \sum_{b=1}^B \kappa_b. \quad (4)$$

Within a branch  $b$  the  $\kappa_b$  companies are assumed to be correlated with a specified correlation coefficient  $C_b$ . To achieve this, the one-factor model adds a part of the branch specific time series  $\eta_{b(k)}(t)$  to the branch independent time series  $\varepsilon_k(t)$ . A sum of these time series is used to construct the asset returns for the companies in the portfolio. The correlated time series  $M_k(t)$  has the form

$$M_k(t) = \sqrt{\frac{p_{b(k)}}{1 + p_{b(k)}}} \eta_{b(k)}(t) + \sqrt{\frac{1}{1 + p_{b(k)}}} \varepsilon_k(t). \quad (5)$$

The entries in both  $\eta_{b(k)}(t)$  and  $\varepsilon_k(t)$  are uncorrelated and standard normal distributed. The weights  $p_{b(k)}$  measure the correlation and satisfy  $p_{b(k)} \geq 0$ . In particular, we have  $p_0 = 0$  for those companies which are in no branch. The normalized, correlated time series  $M_k(t)$  can be arranged in a  $K \times T$  matrix  $M$ , where  $K$  is the number of obligors and  $T$  the length of the time series. The corresponding  $K \times K$  correlation matrix  $C(T)$  is defined as

$$C(T) = \frac{1}{T} M M^\dagger = \langle M_k(t) M_l(t) \rangle_T, \quad (6)$$

where  $M^\dagger$  is the transpose of  $M$ . The index  $T$  on the brackets indicates that the average depends on the length  $T$  of the time series. If the time series are infinitely long, i.e.  $T \rightarrow \infty$ , the correlation coefficient  $C_{kl}(\infty)$  for company  $k$  and  $l$ ,

$$C_{kl}(\infty) = \frac{1}{1 + p_{b(k)}} (p_{b(k)} \delta_{b(k)b(l)} + \delta_{kl}). \quad (7)$$

This value should resemble the best estimate for the correlation and is referred to as the true correlation. The correlation matrix  $C(\infty)$  consists of  $B$  square blocks of dimension  $\kappa_b \times \kappa_b$  at the diagonal. The off-diagonal elements are  $C_b = p_b/(1 + p_b)$  for branch  $b$ , and the no-branch companies are represented by an identity matrix.

TABLE I: Input/output of the model.

Input	Description	Unit
$K$	Number of obligors in the portfolio.	—
$T$	Timespan of the bond (maturity).	Year
$\mu$	Asset drift.	$[\text{Year}]^{-1}$
$\sigma$	Asset volatility.	$[\text{Year}]^{-1/2}$
$\lambda$	Jump intensity.	$[\text{Year}]^{-1}$
$\mu_J$	Mean of the jump size.	Percent
$\sigma_J$	Standard deviation of the jump size.	Percent
$F$	Face value of the bond.	\$
$V_0$	Asset value at the issue date $t = 0$ .	\$
$C$	Correlation matrix.	—
Output	Description	Unit
$P_D$	Probability of default.	Percent
$p(L)$	loss distribution $L$ .	—

All diagonal elements of  $C(\infty)$  are equal to one, and all entries that are not mentioned above are zero. However, for finite length  $T < \infty$ , the true correlations are noise-dressed, because every matrix element carries a random number as offset and the block structure is obscured.

Implementing Noh's model, we are able to analyze a wide range of different portfolio compositions. We emphasize that we automatically include noise, because we work with time series of finite lengths. For this investigation, we find this more realistic because it seems to match the present usage by practitioners. We notice that linear correlations between the asset processes are the simplest form to model the correlations between defaults. They do not account for credit risk contagion across firms and periods of default clustering, see e.g. Refs. [8, 9, 12, 41, 42].

Tab. I summarizes the model parameters and Fig. 4 shows a visualization of the underlying asset value process. The model comprises a large number of parameters. However, this is indispensable if one aims at setting up a realistic model. Credit risk is a problem that involves a high degree of complexity. Importantly, none of our parameters is a hidden parameter. All of them have a direct interpretation and are measurable observables. Thus it is certainly possible to calibrate our model by fitting all parameters to real market data. Admittedly, this task might be time-consuming or even difficult, but it is definitely feasible. A key purpose of the present study is to investigate the tail behavior of the loss distribution. Thus, even if it is difficult to determine some of the parameters sharply, that is, only within some uncertainties, our model yields detailed information on how the tail depends on these parameters.

## B. Related scenarios

The task of finding the probability to hit a certain threshold for an object, a particle, say, whose motion is

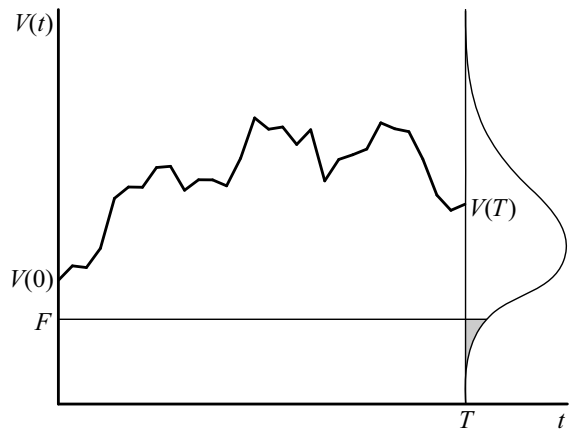


FIG. 4: A visualization of the underlying asset value process, involving the time series of the asset value  $V(t)$  versus time  $t$  with initial value  $V(0) = V_0$ , face value  $F$  and maturity  $T$ . The curve to the right is the distribution of the asset value at maturity. The shaded area corresponds to the default probability.

described by a stochastic process closely relates to the much discussed problem of the stopping time distribution. The stopping time is the time at which the particle hits the threshold. The corresponding distributions are non-trivial objects, because they tend to have non-generic features [43]. This explains the considerable interest which they attract in mathematical statistics.

An application in physico-chemistry is the following: A (Brownian) particle moves stochastically in a suspension confined by a container. It is absorbed when it eventually hits the wall of the container, or it reacts there, or it penetrates the wall if the latter is semipermeable and separates two suspensions. Obviously, the associated loss distribution is very similar to the one in credit risk, if we consider a first passage model. The numerical simulations can be easily adjusted to such a scenario. One could even imagine a force acting between the stochastic particles which would imply a certain correlation between them. However, we do not elaborate on this further, because the purpose of the present discussion is only to establish a qualitative connection.

Another example is a farm where different types of crops are grown. The time evolution of their quality and their future value has a deterministic and a stochastic component. The analogue of default for a given type of crop arises when its value falls below a certain threshold. This could be due to bad weather, diseases, pests, fire, etc., also motivating the inclusion of jump processes. The time series for the crops are correlated, for example, because the diseases are contagious. The knowledge of a distribution for the loss similar to the one in credit risk would be most helpful for the farmer.

The last example shows that the structural model for credit risk can find application in a large number of logistic problems where various objects or quantities have to be available in a certain state at some time in the future.

#### IV. ANALYTICAL DISCUSSION

We investigate a simplified version of our credit risk model analytically. The purposes of this discussion are, first, to illustrate the general mechanisms and, second, to look at the tail behavior. In doing so we demonstrate how and with which speed the loss distribution converges, under certain assumptions, to a universal limit as the number  $K$  of companies is made large. Thus, in this case study, we do not include the jump term in the diffusion process. Moreover, we also make the assumption that the obligors are uncorrelated. We distinguish between individual and portfolio losses in Secs. IV A and IV B.

##### A. Individual losses

The asset value  $V(t)$  for every company  $k$  with  $k = 1, \dots, K$  follows a geometric Brownian motion; its distribution is log-normal. With the initial value  $V(0) = V_0$  at  $t = 0$ , the distribution of  $V(T)$  at maturity  $t = T$  reads

$$p_k(V(T)) = \frac{1}{V(T)\sqrt{2\pi\sigma^2 T}} \exp\left(-\frac{(\ln(V(T)/V_0) - (\mu - \sigma^2/2)T)^2}{2\sigma^2 T}\right). \quad (8)$$

We use the company index only for the distribution  $p_k$ , and we suppress it in the quantities of the asset value process. Due to  $0 \leq V(T) \leq F$  at maturity in the case of default, we have to truncate Eq. (8). Using Eq. (3) we map the distribution of  $V(T)$  to that of the loss given default  $L$  for this company,

$$p_k(L) = \frac{1}{P_D(1-L)\sqrt{2\pi\sigma^2 T}} \exp\left(-\frac{(\ln(F(1-L)/V_0) - (\mu - \sigma^2/2)T)^2}{2\sigma^2 T}\right). \quad (9)$$

The factor needed to restore the normalization,

$$P_D = \frac{1}{2} + \frac{1}{2} \operatorname{erf}\left(\frac{\ln(F/V_0) - (\mu - \sigma^2/2)T}{\sqrt{2\sigma^2 T}}\right), \quad (10)$$

is the default probability for this company  $k$ , where we employ the error function according to the definition

$$\operatorname{erf}(x) = \frac{2}{\sqrt{\pi}} \int_0^x \exp(-\xi^2) d\xi. \quad (11)$$

The number  $P_D$  is the probability that the asset process  $V(t)$  is below the threshold *at* maturity  $T$ , i.e. for having  $V(T) \leq F$ . The default probability is shown in Fig. 4 as shaded area.

The impact of the drift term  $\mu$  and the volatility  $\sigma$  on the default probability is shown in Fig. (5). The range

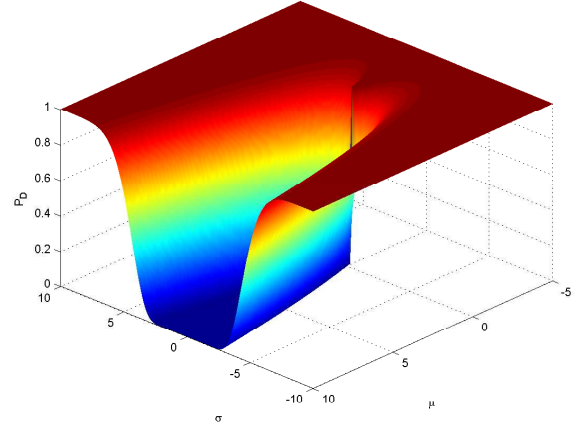


FIG. 5: The default probability (10) as a function of the parameters  $\mu$  and  $\sigma$  for the values  $V_0 = 100$ ,  $F = 75$  and  $T = 1$ . The default probability tends to increase rapidly when choosing parameter values that are too large. Also one can see that it is an even function in  $\sigma$ , indicating that it is only the absolute value that matters.

in which realistic default probabilities are generated is very narrow, both in the  $\mu$  and  $\sigma$  direction. For our simulations we choose  $\mu = 0.05$  and  $\sigma = 0.15$ , which results in a default probability of  $P_D \approx 0.0148$ .

For later purposes, we calculate the  $n$ -th moment

$$\langle L_k^n \rangle = \int_0^1 L^n p_k(L) dL \quad (12)$$

of the distribution (9). By using the index  $k$  in our notation, we want to underline that the  $\langle L_k^n \rangle$  are the moments of the distribution for the *individual* loss given default. We arrive at

$$\begin{aligned} \langle L_k^n \rangle &= \frac{1}{2P_D} \sum_{j=0}^n (-1)^j \binom{n}{j} \\ &\exp\left(j(j-1)\frac{\sigma^2}{2}T + j\left(\mu T - \ln\frac{F}{V_0}\right)\right) \\ &\left(1 + \operatorname{erf}\left(\frac{(1-2j)\sigma^2 T/2 - \mu T + \ln(F/V_0)}{\sqrt{2\sigma^2 T}}\right)\right) \end{aligned} \quad (13)$$

after a straightforward calculation.

##### B. Portfolio losses

The loss  $L$  of the total portfolio is the arithmetic mean of the individual losses,

$$L = \frac{1}{K} \sum_{k=1}^K L_k I_k, \quad (14)$$

where  $L_k$  is the loss given default for the individual bond with index  $k$  and  $K$  is the total number of bonds in the

portfolio. As we are interested in the distribution of the portfolio loss, we have to introduce the default indicator  $I_k$  for company  $k$  by

$$I_k = \begin{cases} 1 & , \text{ if } V(T) < F \quad (\text{default}) \\ 0 & , \text{ if } V(T) > F \quad (\text{no default}) \end{cases} \quad (15)$$

As the distribution of the default indicator for company  $k$ , we choose

$$\tilde{p}_k(I_k) = (1 - P_D)\delta(I_k) + P_D\delta(I_k - 1) . \quad (16)$$

The default probability (10) depends on the specific parameters which go into the asset value process for company  $k$ . To obtain the distribution of the portfolio loss we have to average over all distributions of the individual losses  $p_k(L_k)$ , given by Eq. (9), and over the indicator distributions (16),

$$\begin{aligned} p(L) &= \int_{-\infty}^{+\infty} dI_1 \tilde{p}_1(I_1) \cdots \int_{-\infty}^{+\infty} dI_K \tilde{p}_K(I_K) \\ &\quad \int_0^1 dL_1 p_1(L_1) \cdots \int_0^1 dL_K p_K(L_K) \\ &\quad \delta\left(L - \frac{1}{K} \sum_{k=1}^K L_k I_k\right) . \end{aligned} \quad (17)$$

We notice the subtle difference between the loss distribution and the distribution of the loss given default. This difference is best understood by considering Eq. (17) for  $K = 1$ , which yields

$$p(L) = (1 - P_D)\delta(L) + P_D p_1(L) . \quad (18)$$

This is the weighted sum of the distributions for the case of no default and for the case of default.

We calculate an asymptotic approximation to  $p(L)$  for a large number  $K$  of companies, i.e. for large portfolio size. Here, we make the further assumptions that the face values and the parameters of the geometric Brownian motion are the same for all companies  $k$ . These additional assumptions are not strictly necessary for the feasibility of the calculation, but they make the resulting expressions very compact. Details of the computation are given in Appendix A. We obtain

$$\begin{aligned} p(L) &\approx \frac{1}{2\pi} \int_{-\infty}^{+\infty} d\omega \exp(-i\omega(L - P_D\langle L_k \rangle)) \\ &\quad \exp\left(-\frac{\omega^2}{2K} (P_D\langle L_k^2 \rangle - P_D^2\langle L_k \rangle^2)\right) \\ &\quad \exp\left(-\frac{i\omega^3}{6K^2} (P_D\langle L_k^3 \rangle \right. \\ &\quad \left. + 3P_D^2\langle L_k \rangle\langle L_k^2 \rangle + 2P_D^3\langle L_k \rangle^3)\right) , \end{aligned} \quad (19)$$

as asymptotic approximation to order  $1/K^2$ . If we skip the  $1/K^2$  term and settle with an  $1/K$  expansion, we find the shifted Gaussian

$$\begin{aligned} p(L) &\approx \sqrt{\frac{K}{2\pi(P_D\langle L_k^2 \rangle - P_D^2\langle L_k \rangle^2)}} \\ &\quad \exp\left(-\frac{K(L - P_D\langle L_k \rangle)^2}{2(P_D\langle L_k^2 \rangle - P_D^2\langle L_k \rangle^2)}\right) . \end{aligned} \quad (20)$$

Thus, the Central Limit Theorem applies if the number  $K$  of companies is very large. The expected loss EL, i.e. the peak position, is the mean value of  $L_k$ , weighted with the default probability  $P_D$ . This is so, because we defined the portfolio loss  $L$  as the arithmetic mean (14). The unexpected loss UL quantifying the risk is given by the square root of  $(P_D\langle L_k^2 \rangle - P_D^2\langle L_k \rangle^2)/K$  which becomes smaller with  $K$ . Even in the Gaussian limit, the dependence of  $p(L)$  on the parameters  $F$ ,  $V_0$ ,  $\mu$ ,  $\sigma$  and  $T$  is non-trivial due to the rather involved expressions (10) for the default probability and (13) for the moments. We will return to this point. Due to the specific nature of the approximation that leads to Eq. (19), the first moments of the exact distribution are preserved up to the highest order of  $\omega$  which is considered in the exponential. Therefore, Eq. (19) contains the correct first, second and third moment, while the Gaussian limit in Eq. (20) still has the correct mean and variance.

Further, it is important to note that expression (19) holds for any structural model for uncorrelated and homogenous portfolios, i.e. with all face values and parameters of the geometric Brownian motion being the same for all companies  $k$ . It does not depend on the choice of random processes for the asset values  $V(t)$ , and it is sufficient to know the default probability and the first three moments of the individual loss given default distribution. It is straightforward to generalize Eq. (19) to the case of inhomogenous portfolios (see Appendix B).

### C. Exact loss distribution versus approximations

The approximation in the previous subsection has the advantage of being easily extendable to more general portfolios and exactly conserving the first moments of the distribution up to the order of approximation. However, it does not reproduce the shape and, in particular, the tail behavior very well.

A better approximation of the loss distribution is possible, if we restrict ourselves again to homogenous portfolios. Using the default indicator function defined in Eq. (16), we can then rewrite Eq. (17) as a combinatorial sum

$$p(L) = \sum_{j=0}^K \binom{K}{j} (1 - P_D)^{K-j} P_D^j F_j(L) \quad (21)$$



where we define the function  $F_j(L)$  as

$$\begin{aligned}
 F_j(L) &= \int_0^1 dL_1 p_1(L_1) \cdots \int_0^1 dL_j p_j(L_j) \\
 &\quad \delta\left(L - \frac{1}{K} \sum_{k=1}^j L_k\right) \\
 &\approx \frac{1}{2\pi} \int_{-\infty}^{\infty} d\omega \exp\left(-i\omega\left(L - \frac{j}{K}\langle L_k \rangle\right)\right) \\
 &\quad \exp\left(-\frac{\omega^2 j}{2K^2} (\langle L_k^2 \rangle - \langle L_k \rangle^2)\right) \\
 &\quad - \frac{i\omega^3 j}{6K^3} (\langle L_k^3 \rangle - 3\langle L_k \rangle \langle L_k^2 \rangle + 2\langle L_k \rangle^3) \Bigg).
 \end{aligned} \tag{22}$$

The approximation for  $F_j(L)$  follows the same line of arguing which is outlined in Appendix A. Note that each term of the sum in Eq. (21) corresponds to the event that exactly  $j$  defaults occur. In particular, for  $j = 0$  the delta peak  $(1 - P_D)^K \delta(L)$  is obtained exactly in this approximation.

In Figure 6 we compare the exact loss distributions for  $K = 10, 100$  and  $1000$  to the asymptotic approximation (19) to order  $1/K^2$ , and to Eq. (21) with the approximation in Eq. (22). In both cases, the analytical approximations are evaluated numerically. The exact loss distributions are obtained by calculating numerically the convolutions in Eq. (22), using the characteristic function of  $p_k(L)$ , and inserting these  $F_j(L)$  into Eq. (21). As numerical values for the model parameters we choose  $\mu = 0.05$ ,  $\sigma = 0.15$ ,  $T = 1$ ,  $V_0 = 100$  and  $F = 75$ .

For  $K = 10$  the delta peak  $(1 - P_D)^K \delta(L)$  (not shown in the plots) is quite dominant and leads to a very poor result of approximation (19), while the approximation of Eq. (21) already yields a quite reasonable result. For  $K = 100$ , features of the Gaussian limit are already present. Pictorially speaking, the Gaussian moves from the left into the picture. The approximation of Eq. (21) captures the tail behavior of the distribution quite nicely.

For  $K = 1000$ , the Gaussian limit (20) is almost reached, but, interestingly, the distribution is still slightly asymmetric. The agreement with the asymptotic approximation (19) is convincing, although the tail behavior is not as well described as by the approximation of Eq. (21).

Figure 6 yields a good intuition for the tail behavior and for the speed of convergence to the Gaussian, or any other universal limit. Remarkably, even for  $K = 1000$  slight deviations from the Gaussian are seen. This means that, importantly, only really large portfolio sizes imply universal shapes.

A measure for the tail behavior of the loss distribution is the kurtosis, which is defined as a normalized form of the forth central moment  $\mu_4$

$$\beta_2 = \frac{\mu_4}{\mu_2^2}, \tag{23}$$

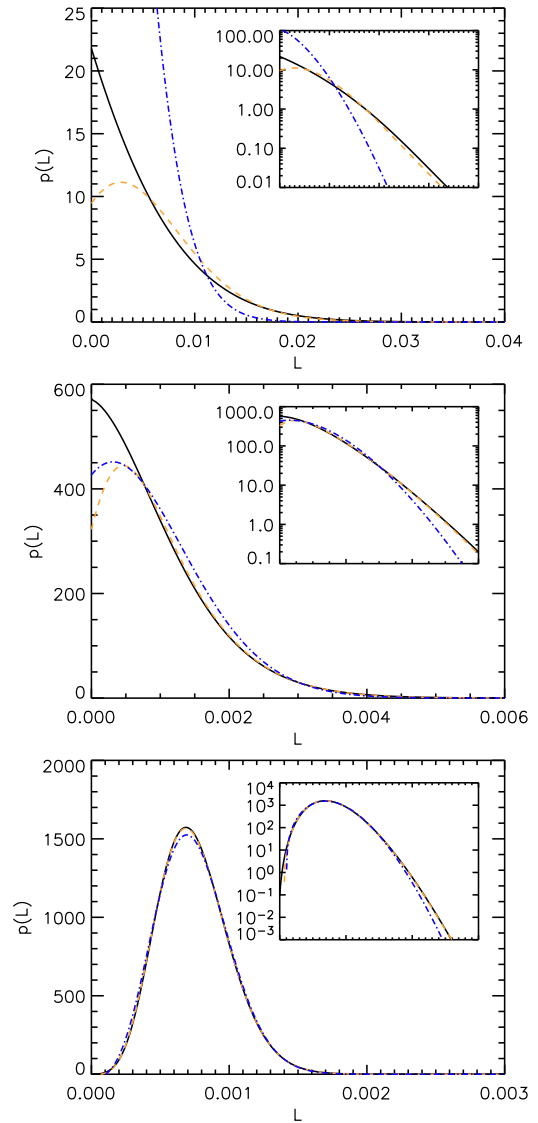


FIG. 6: Loss distribution for three different portfolio sizes  $K = 10, 100, 1000$ , respectively. The insets show logarithmic plots. Black solid lines show the analytical results, while the blue dashed-dotted lines correspond to Eq. (19), and the orange dashed lines to the approximation of Eq. (21). The model parameters are  $\mu = 0.05$ ,  $\sigma = 0.15$ ,  $T = 1$ ,  $V_0 = 100$  and  $F = 75$ .

where  $\mu_2$  is the second central moment. Since the kurtosis of the normal distribution is equal to three, the *kurtosis excess* is defined as

$$\gamma_2 = \frac{\mu_4}{\mu_2^2} - 3. \tag{24}$$

It can be shown analytically that the kurtosis excess for homogenous and uncorrelated portfolios is proportional to  $1/K$ . Such considerations are important in modern portfolio theory, for example, when one tries to minimize risk by diversification. This can require an enlargement of the portfolio.

We notice that the symmetric shape of the Gaussian can only be reached without correlations between the asset processes: with correlations, the probability of default is enlarged without compensation on the positive side, because in the best case, none of the obligors defaults. Thus, the distribution is asymmetric.

#### D. Drill down risk

Consider a portfolio consisting of  $K$  companies. The moments of the loss given default distribution are assumed to be known. In which way will the properties of the portfolio change if one decides to add or remove a company? If one had this information an optimal strategy could be developed to drill down the parts within the portfolio which are the most risky, or to decide which new company should be added, so that the additional risk is minimal.

Since we want to allow the individual face values  $F_k$  and the initial values  $V_{0k}$  to be different now, it would be unsuitable to use the dimensionless definition (14) of the losses. Instead we use a more general definition of the individual loss

$$\Gamma_k \equiv L_k F_k = F_k - V_k(T), \quad (25)$$

which now has the dimension of dollars. The *total loss* for the entire portfolio of size  $K$  is then

$$L^{(K)} = \frac{\sum_{k=1}^K \Gamma_k I_k}{\sum_{k=1}^K F_k}, \quad (26)$$

which again is a normalized quantity with  $0 \leq L^{(K)} \leq 1$ .  $I_k$  is the indicator function for company  $k$ , as defined in Eq. (15). If *all* face values  $F_k$  are the same,  $F_k = F$ , the loss will again reduce to Eq. (14), since

$$L^{(K)} = \frac{\sum_{k=1}^K \Gamma_k I_k}{\sum_{k=1}^K F_k} = \frac{F_k \sum_{k=1}^K L_k I_k}{K F_k} = \frac{1}{K} \sum_{k=1}^K L_k I_k. \quad (27)$$

Now, is it possible to express the moments of the loss distribution for  $K$  companies, in terms of the corresponding loss distribution for  $K-1$  companies? Indeed it is. See Appendix C for details. The  $n$ :th moment can be expressed as:

$$\begin{aligned} \left\langle \left( L^{(K)} \right)^n \right\rangle_K &= \left( \frac{F^{(K-1)}}{F^{(K)}} \right)^n \\ &\times \sum_{\nu=0}^n \binom{n}{\nu} \left\langle \left( L^{(K-1)} \right)^{n-\nu} \right\rangle_{K-1} \\ &\times \frac{\langle I_K^\nu \rangle \langle \Gamma_K^\nu \rangle}{(F^{(K-1)})^\nu}, \end{aligned} \quad (28)$$

where  $\nu$  is an integer and  $F^{(K)}$  is the sum over all the  $K$  face values:

$$F^{(K)} = \sum_{j=1}^K F_j. \quad (29)$$

For example, the two first moments are, for  $n=1$

$$\begin{aligned} \left\langle \left( L^{(K)} \right) \right\rangle_K &= \frac{F^{(K-1)}}{F^{(K)}} \left\langle \left( L^{(K-1)} \right) \right\rangle_{K-1} \\ &+ \frac{1}{F^{(K)}} \langle I_K \rangle \langle \Gamma_K \rangle, \end{aligned} \quad (30)$$

and for  $n=2$

$$\begin{aligned} \left\langle \left( L^{(K)} \right)^2 \right\rangle_K &= \left( \frac{F^{(K-1)}}{F^{(K)}} \right)^2 \left\langle \left( L^{(K-1)} \right)^2 \right\rangle_{K-1} \\ &+ 2 \frac{F^{(K-1)}}{(F^{(K)})^2} \langle I_K \rangle \langle \Gamma_K \rangle \left\langle \left( L^{(K-1)} \right) \right\rangle_{K-1} \\ &+ \frac{1}{(F^{(K)})^2} \langle I_K^2 \rangle \langle \Gamma_K^2 \rangle. \end{aligned} \quad (31)$$

#### V. NUMERICAL DISCUSSION

The numerical analysis of our model is done with Monte Carlo simulations. To achieve results that are statistically reliable, we simulated between  $10^4$  and  $10^5$  asset processes. An important remark is in order. Given the rich variety of credit contracts, we decided not to calibrate our model with real market data, because this would match only one particular scenario. However, we have chosen the parameter values in such a way [16] that the model outcome is economically realistic. In particular, the parameters of the jump process have been chosen in order to reproduce a realistic tail behavior. For homogenous and uncorrelated portfolios the loss distributions obtained by the Monte Carlo simulations agree very well with the analytical expectation. In Sec. V A we study the impact of maturity, drift and volatility. Leverage, jumps and correlations are addressed in Secs. V B, V C and V D, respectively. We discuss the competition between jumps and correlations in Sec. V E.

##### A. Maturity, drift and volatility

To give the reader a better feeling for the sensitivity of the loss distribution, we first take a look at the model in its simplest form, i.e without jumps and correlations, and study its dependence on maturity  $T$ , drift  $\mu$  and volatility  $\sigma$ . This is again done by calculating Eq. (21) numerically, while in the remainder of the paper we use Monte Carlo simulations.

We begin with the maturity  $T$  and keep  $\mu = 0.05$ ,  $\sigma = 0.15$ ,  $V_0 = 100$  and  $F = 75$ . It is quite common that loans span over a period longer than  $T = 1$  year which has been considered so far. In Fig. 7, the expected loss EL and the unexpected loss UL are shown as a function of maturity  $T$ . The expected loss EL is the mean value  $P_D \langle L_k \rangle$  and the unexpected loss UL squared is the variance  $(P_D \langle L_k^2 \rangle - P_D^2 \langle L_k \rangle^2)/K$ , where the default probability  $P_D$  and the moments  $\langle L_k^n \rangle$  are given by Eqs. (10) and (13). Closer

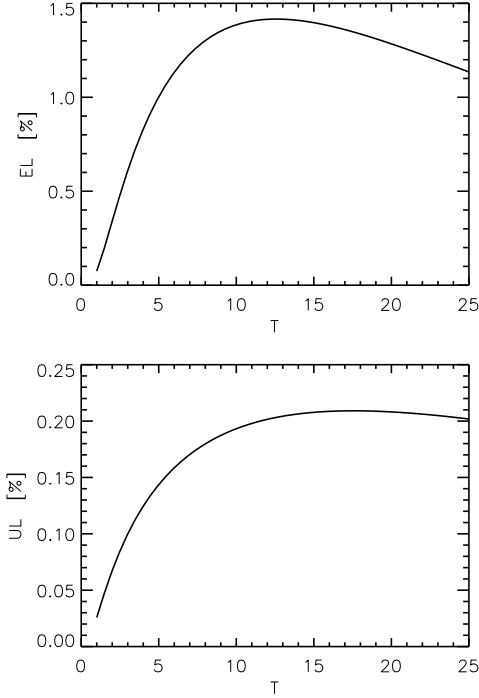


FIG. 7: Expected loss EL and unexpected loss UL as a function of the maturity  $T$  for  $K = 1000$ .

inspection shows that EL grows monotonically in  $T$  to its saturation value unity, if, for fixed (positive) drift  $\mu$  and volatility  $\sigma$ , the condition  $\mu < \sigma^2/2$  is met. However, if  $\mu > \sigma^2/2$ , EL has a maximum for some finite value of  $T$  and the saturation value of EL is zero for  $T \rightarrow \infty$ . For the parameter choices  $\mu = 0.05$  and  $\sigma = 0.15$ , the maximum is at  $T \approx 12.56$ , as seen in Fig. 7. Similar considerations apply to UL, with the maximum at  $T \approx 17.55$ .

In the sequel, we put  $T = 1$  and investigate the dependence on drift  $\mu$  and volatility  $\sigma$ . We choose  $0.05 \leq \mu \leq 0.15$  and  $0.15 \leq \sigma \leq 0.35$  which is motivated by economical data. The expected loss EL and the unexpected loss UL for  $K = 1000$  are depicted in Fig. 8. For  $K = 1$  (not shown), both EL and UL are proportional to the volatility and only weakly dependent on the drift. For portfolio sizes  $K > 1$  and fixed volatility  $\sigma$ , both EL and UL increase with decreasing  $\mu$ . This reflects that the probability to default increases with smaller  $\mu$ . Importantly, the loss distribution becomes more sensitive to this effect with growing portfolio size. This is so, because the portfolio loss is an average of individual losses. The expected loss EL and the unexpected loss UL increase with volatility. As for the drift, the sensitivity of the loss distribution to the volatility grows with the portfolio size. A larger volatility implies larger asset returns which cause a greater activity of the asset value. This, in turn, produces excessive losses.

We conclude that the qualitative behavior of the loss distribution as function of drift and volatility is very similar. Economically, this means that a downwards change

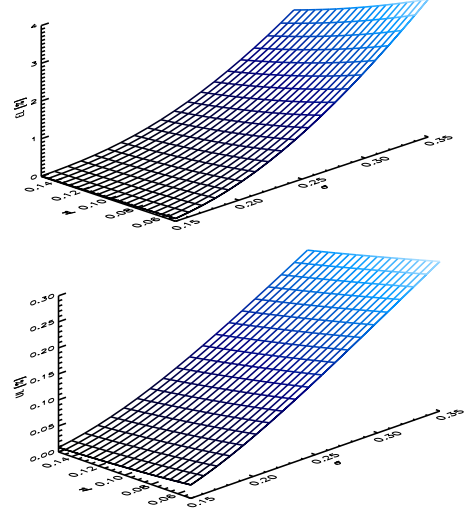


FIG. 8: Expected loss EL and unexpected loss UL as a function of the drift  $\mu$  and the volatility  $\sigma$  for  $K = 1000$ .

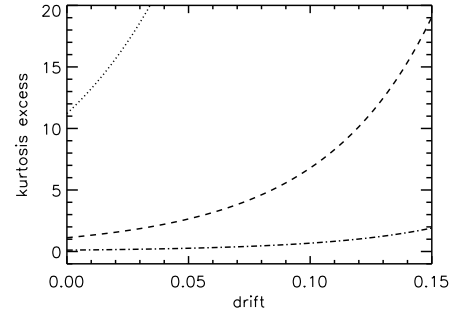


FIG. 9: The kurtosis excess as a function of the asset drift  $\mu$  for portfolio sizes  $K = 10$  (dotted),  $K = 100$  (dashed) and  $K = 1000$  (dashed-dotted).

in the general trend of the asset prices during a quiet, not volatile period affects the credit markets in a similar way as an upwards change in the market activity, i.e. volatility, in times of a stable general trend in the markets. According to Eq. (10), the default probability is almost proportional to both drift and volatility in the parameter range chosen.

Finally, we study how drift  $\mu$  and volatility  $\sigma$  affect the tail behavior of the loss distribution. We recall that the universal limit is in the present case always Gaussian for very large  $K$ . It can be shown analytically that the kurtosis excess of uncorrelated portfolios scales as  $1/K$ . Figures 9 and 10 show the kurtosis excess as functions of drift and volatility, respectively. In Fig. 9 one sees that a higher drift gives loss distributions with fatter tails. This is more pronounced for large portfolio sizes. Figure 10 shows that the kurtosis excess approaches zero, i.e. the distribution becomes more Gaussian, with grow-

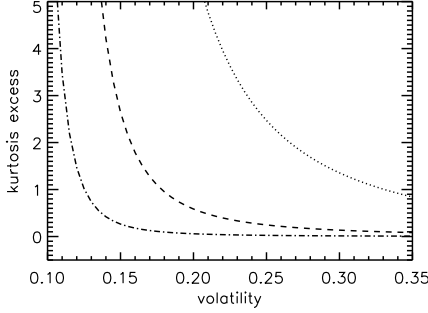


FIG. 10: The kurtosis excess as a function of the asset volatility  $\sigma$  for portfolio sizes  $K = 10$  (dotted),  $K = 100$  (dashed) and  $K = 1000$  (dashed-dotted).

ing volatility. Moreover, one also observes that the speed of convergence to a Gaussian is higher for larger portfolio size, which reflects the Central Limit Theorem.

### B. Leverage

The ratio  $F/V_0$  between the face value of the bond  $F$  and the initial asset value  $V_0$  is referred to as leverage. It is very important for credit risk managers to know its influence on the loss distribution. In our model we are able to set both the face value of the bond and the initial asset value. However, as it suffices to study only the leverage, we keep  $V_0 = 100$  fixed and only vary the face value  $F$ . The portfolio default probability PD, expected loss EL and the unexpected loss UL grow with the leverage. This is so, because the higher the leverage, the more likely are early defaults. It is a remarkable result that large portfolios are extremely sensitive to the leverage. As every realistic portfolio contains bonds with different leverage, it is of considerable interest to study how the loss distribution changes if the leverages are distributed. Here, the (relative) loss  $L$  is defined as the sum of the absolute losses  $F_k L_k I_k$  divided by the sum of the face values  $F_k$  of the companies  $k = 1, \dots, K$ . Here  $L_k$  is the (relative) loss given default for company  $k$  and  $I_k$  the corresponding default indicator. For convenience, we choose uniform distributions with width  $\Delta F$  centered around  $F = 75$ . The results are shown in Fig. 11. Expected loss EL and unexpected loss UL grow with  $\Delta F$ .

### C. Jumps

The need to include jumps in a realistic model has been pointed out in Sec. III A. Jumps are important despite the fact that the jump intensity is typically very small. Reasonable economical values of the jump intensity are around 0.01 jumps per year. If not otherwise stated, we use the following values for the jump process: jump intensity  $\lambda = 0.01$ , mean jump size  $\mu_J = -0.4$ ,

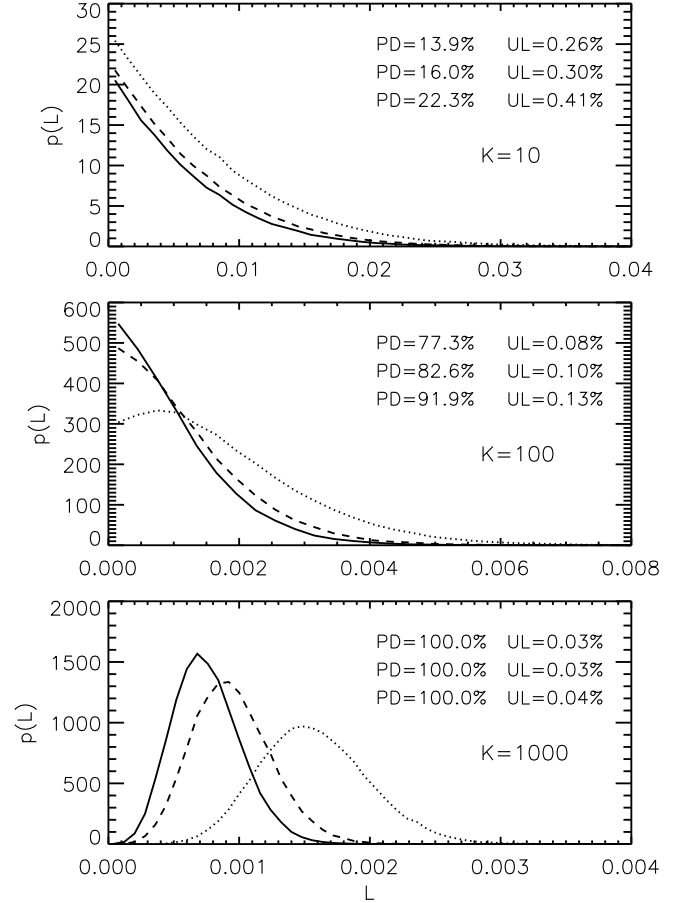


FIG. 11: Loss distributions for portfolios in which the leverage is uniformly distributed. The face values are random in a window of width  $\Delta F$  around  $F = 75$  with  $\Delta F = 0$  (solid lines),  $\Delta F = 10$  (dashed lines) and  $\Delta F = 20$  (dotted lines), for three different portfolio sizes  $K = 10, 100, 1000$ , respectively. The expected loss EL is 0.076%, 0.095% and 0.157% for the three different leverages (independent of  $K$ ). The insets show, for every portfolio size, the portfolio default probability PD and the unexpected loss UL from top to bottom for  $\Delta F = 0, 10, 20$ .

and standard deviation  $\sigma_J = 0.3$ . In Fig. 12 we plot the loss distributions for three different jump intensities,  $\lambda = 0.005, 0.01, 0.015$ . Not surprisingly, PD, EL and UL increase with the jump intensity. As for any uncorrelated portfolio, EL is independent of the portfolio size, while UL scales with  $1/\sqrt{K}$ . For  $K = 1000$ , PD has already saturated at 100%. In Figure 13 the kurtosis excess is depicted as a function of the jump intensity  $\lambda$ . The kurtosis excess grows with the jump intensity up to a certain value of the intensity, then it decreases again and approaches zero asymptotically. For larger values of  $\lambda$ , the loss distribution is more smeared out, because the losses produced by the jumps dominate the defaults due to the standard geometric Brownian motion. In other words, the emergence of the maximum can be explained

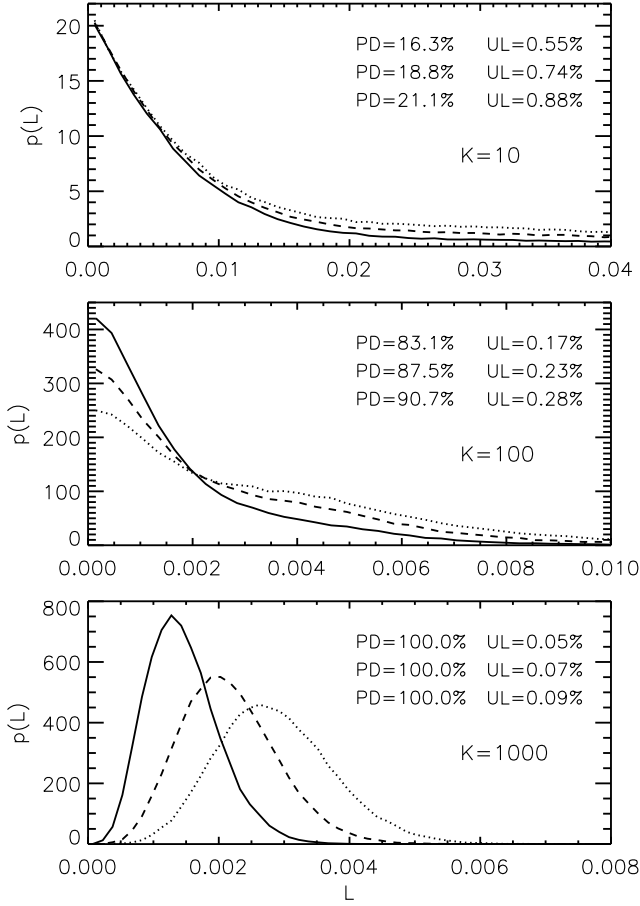


FIG. 12: Loss distributions for portfolios with different jump intensities  $\lambda = 0.005$  (solid lines),  $\lambda = 0.01$  (dashed lines) and  $\lambda = 0.015$  (dotted lines) for four different portfolio sizes  $K = 10, 100, 1000$ , respectively. The expected loss EL is 0.15%, 0.22% and 0.29% for the three different jump intensities. The insets show, for every portfolio size, the portfolio default probability PD and the unexpected loss UL from top to bottom for  $\lambda = 0.005, 0.01, 0.015$ .

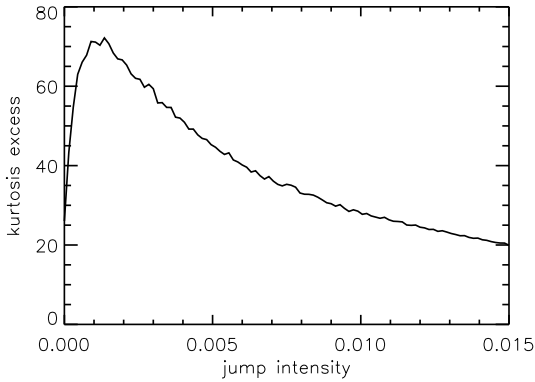


FIG. 13: The kurtosis excess as a function of the jump intensity  $\lambda$ . The result is shown for  $K = 10$ , and it scales with  $1/K$ .

as follows. The kurtosis is high for a distribution that has a sharp peak around the mean and a fat tail. When the intensity  $\lambda$  grows starting from  $\lambda = 0$ , the tail becomes fatter, because the kurtosis increases. But at some value of  $\lambda$ , the tail becomes so heavy that it interferes with and ultimately destroys the sharp peak of the distribution. Hence, the kurtosis excess must have a maximum value for some intensity  $\lambda$ . Furthermore, we notice that the kurtosis excess scales as  $1/K$  with the portfolio size.

As discussed in Sec. III A, we make the specific assumption that the distribution of the jump sizes is log-normal. Hence, it is important to see how the loss distributions depend on the parameters of the jump size distribution. The losses grow when the absolute value of the jump mean  $\mu_J$  increases. This is illustrated in Fig. 14. As for the jump intensity, the sensitivity of the loss distribution to the jump mean does not significantly depend on the portfolio size. Furthermore, as displayed in Fig. 15, the credit losses slightly increase, for all portfolio sizes, with the jump size standard deviation  $\sigma_J$ .

#### D. Correlations

To begin with, we choose the simplest possible correlation matrix  $C = C(T)$ , i.e. a portfolio where all companies are in the same branch. Figure 16 shows the structure of the correlation matrix and the loss distributions for different portfolio sizes and branch correlations  $c = C_b$ . In the sequel, the structure of the correlation matrix is always presented as a gray scale image where the intensity corresponds to the correlation. Black areas stand for unit correlation, white areas for zero correlation. The expected loss EL is 0.076% for all three branch correlations, i.e. it is independent of the branch correlation and, as in the case of uncorrelated portfolios, it is also independent of the portfolio size. The unexpected loss UL becomes larger as the branch correlation grows, while the portfolio default probability PD decreases. The latter can be understood, because the portfolio increasingly acts as a single company with growing correlation strength. The portfolio default probability makes a transition from  $1 - (1 - P_D)^K$ , corresponding to  $K$  uncorrelated companies ( $c = 0$ ), to  $P_D$  for a single company ( $c = 1$ ).

Figure 16 shows that, as for a majority of the model parameters, the impact of the correlation on the loss distribution increases with the portfolio size. Remarkably, there is a sizable deviation from a Gaussian-type-of shape. This is seen in Fig. 17 which shows the kurtosis excess of the loss distribution as a function of the branch correlation  $c = C_b$  for this one-branch scenario. The kurtosis excess for a portfolio of size  $K$  shows a transition from the value  $264.6/K$  for an uncorrelated portfolio ( $c = 0$ ) to 264.6, which corresponds to the value for an individual obligor. Between  $c = 0.6$  and  $c = 1$  the kurtosis excess even exceeds this value. To gain further insight into the influence of correlations, we now assume that the

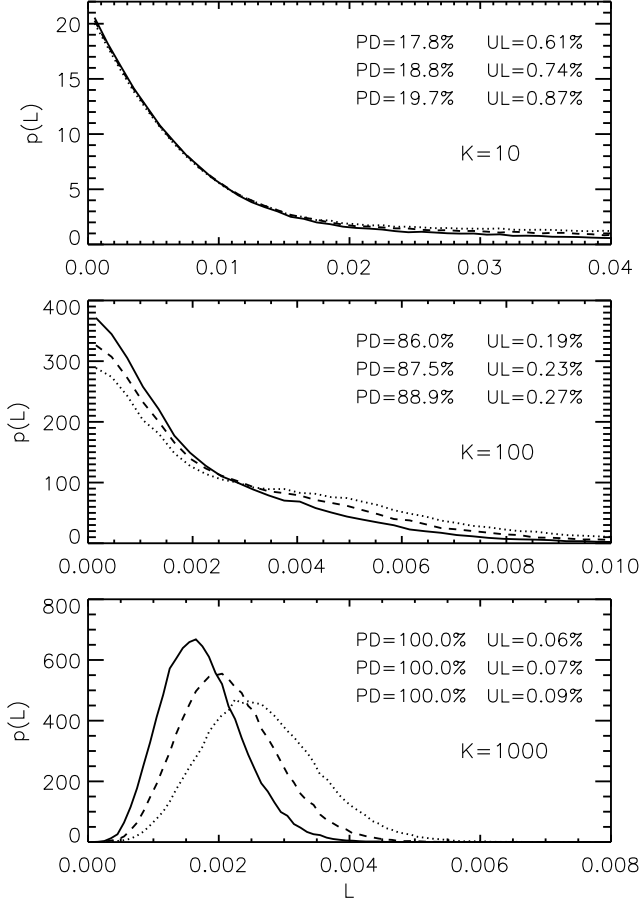


FIG. 14: Loss distributions for portfolios with different mean values of the jump size,  $\mu_J = -0.3$  (solid lines),  $\mu_J = -0.4$  (dashed lines) and  $\mu_J = -0.5$  (dotted lines) for four different portfolio sizes  $K = 10, 100, 1000$ , respectively. The standard deviations is always  $\sigma_J = 0.3$ . The expected loss EL is 0.18%, 0.22% and 0.26%, and the portion of negative jumps are 86%, 91% and 94% for the three  $\mu_J$  values, respectively. The insets show, for every portfolio size, the portfolio default probability PD and the unexpected loss UL from top to bottom for  $\mu_J = -0.3, -0.4, -0.5$ .

size  $\kappa_1$  of the branch is smaller than the total size  $K$  of the correlation matrix. Thus,  $\kappa_1$  companies are correlated,  $K - \kappa_1$  are not. In Fig. 18 we plot loss distributions for different branch sizes  $\kappa_1$ , the branch correlation is  $c = C_b = 0.5$ . We observe that bigger branch size yields a higher unexpected loss UL and a lower portfolio default probability PD. Importantly, the loss distributions for  $K = 1000$  show a transition from a strongly leptokurtic to a more Gaussian-type-of, but still asymmetric, distribution as  $\kappa_1$  decreases. This clearly visualizes the effect already mentioned in Sec. IV A. A symmetric Gaussian-type-of shape can only be reached without correlations between the asset processes.

In a realistic economical scenario, companies will belong to  $B$  different branches. In Fig. 19, results are de-

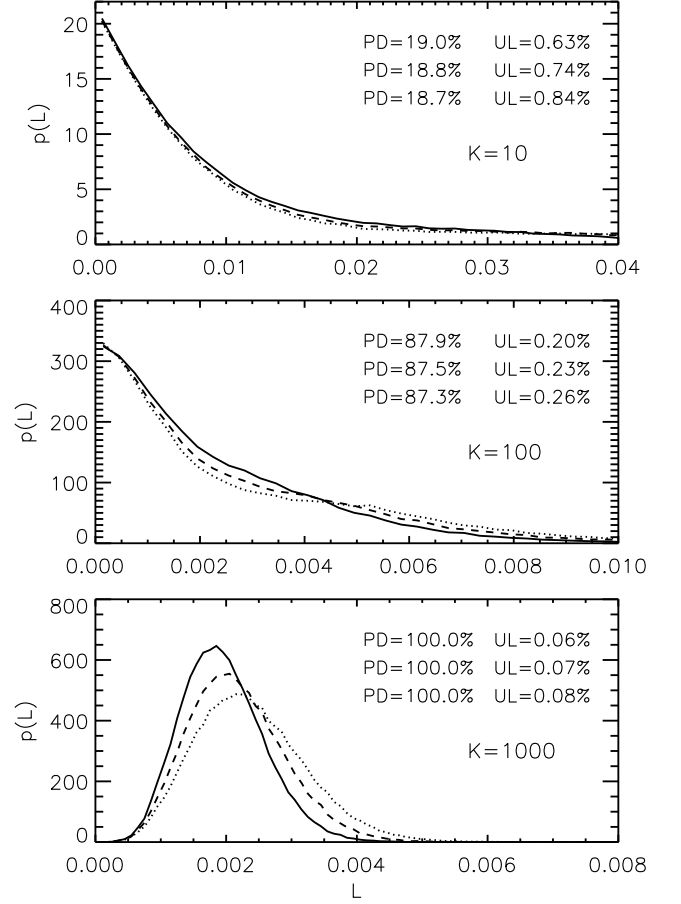


FIG. 15: Loss distributions for portfolios with different standard deviations  $\sigma_J$  of the jump size.  $\sigma_J = 0.2$  (solid lines),  $\sigma_J = 0.3$  (dashed lines) and  $\sigma_J = 0.4$  (dotted lines) for three different portfolio sizes  $K = 10, 100, 1000$ , respectively. The mean is always  $\mu_J = -0.4$ . The expected loss EL is 0.20%, 0.22% and 0.24%, and the portion of negative jumps are 96%, 91% and 87% for these  $\sigma_J$ . The insets show, for every portfolio size, the portfolio default probability PD and the unexpected loss UL from top to bottom for  $\sigma_J = 0.2, 0.3, 0.4$ .

picted for portfolios consisting of companies in  $B = 1, 2, 5$  branches, all with the same branch correlation  $c = C_b = 0.5$ . The structure of the correlation matrices is also shown in the figure. The number of branches does not significantly affect the loss distribution. Moreover, the loss distribution does not approach the normal distribution as the size of the portfolio increases. This is so, because the high branch correlation  $c = C_b = 0.5$  makes the branches in the portfolio behave like individual companies. Hence, the  $K \times K$  correlation matrix is effectively only  $B \times B$ . The curves in the subfigures of Fig. 19 are almost identical, since for high  $c = C_b$  there is no significant difference between portfolios containing one, two or five companies.

An interesting question is whether a small, highly correlated branch has more or less effect than a large branch

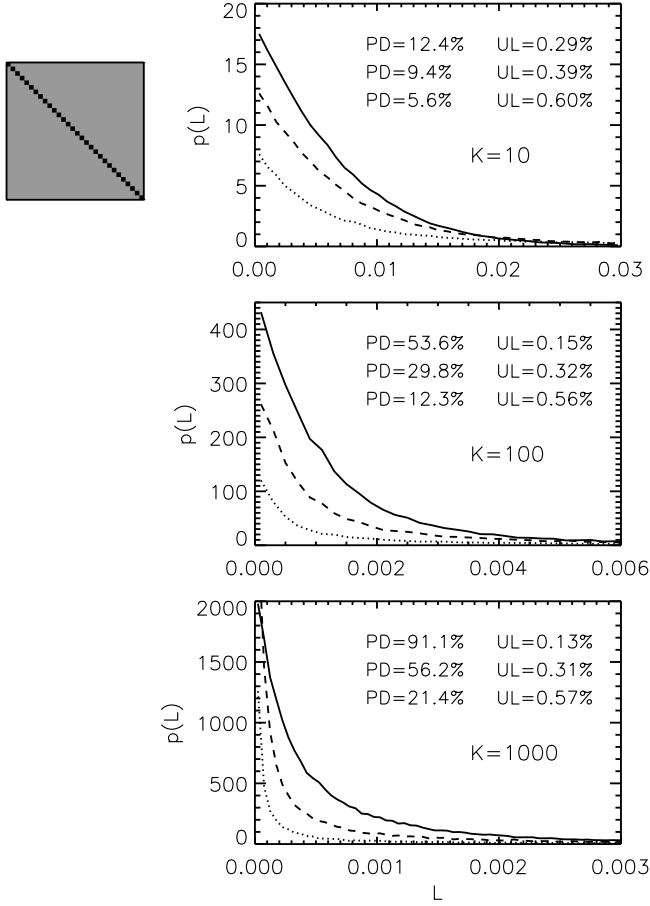


FIG. 16: Loss distributions for portfolios with different branch correlations. The top left plot shows the structure of the correlation matrix, all companies are in one branch, indicated in grey. The other three plots show the loss distributions for three different portfolio sizes  $K = 10, 100, 1000$ , respectively. The correlations are measured by the branch correlation parameter  $c = 0.2$  (solid lines),  $c = 0.5$  (dashed lines) and  $c = 0.8$  (dotted lines). The expected loss is 0.076% for all three branch correlations, i.e. it is independent of the branch correlation. The insets show, for every portfolio size, the portfolio default probability PD and the unexpected loss UL from top to bottom for  $c = 0.2, 0.5, 0.8$ .

with weakly correlated companies. To look into this, we investigate how the loss distribution depends on the product  $\kappa_1 c$  of the branch size  $\kappa_1$  and the branch correlation  $c = C_b$ . Figure 20 shows loss distributions for portfolios where 90%, 50% and 10% of the obligors in the portfolio are in a branch. The correlations for these branches are 0.1, 0.18 and 0.9 respectively. Thus, the product is  $\kappa_1 c = 9$  in all three cases. We notice that  $\kappa_1$  denotes the branch size in percent of the total number  $K$  of obligors. We conclude that a small, highly correlated branch and a larger branch with less correlated companies are equivalent from a creditor's point of view. The unexpected loss UL is very similar, although not identical, for the three different parameter settings, while the portfolio default

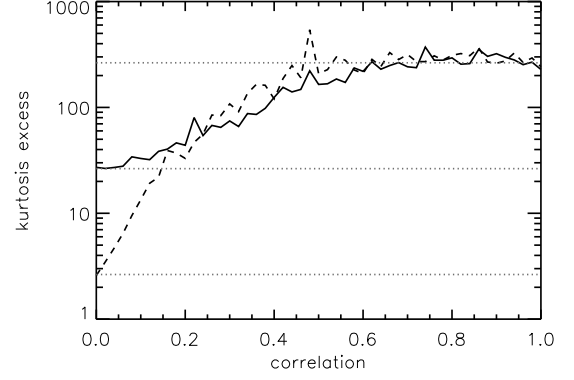


FIG. 17: The kurtosis excess as a function of the correlation parameter  $c$  for portfolio sizes  $K = 10$  (solid line) and  $K = 100$  (dashed line). The horizontal dotted lines indicate the kurtosis excess of the corresponding uncorrelated portfolios,  $264.6/K$ , for  $K = 1, 10$  and  $100$ , respectively.

probability PD is decreasing with increasing  $\kappa_1$ . The effect on PD is observed to be strongest for intermediate size portfolios ( $K = 100$  in our case).

### E. Jumps versus correlations

Here, we study the interplay between jumps and correlations. In Figs. 21 and 22 the portfolio default probability PD and the unexpected loss UL are displayed as functions of the jump intensity  $\lambda$  and the branch correlation  $c$ . To keep the discussion transparent, the correlation structure is a single branch containing all companies. The portfolio default probability PD increases with the jump intensity and decreases with growing correlation. For fixed small jump intensity  $\lambda$  both PD and UL show a transition from  $K$  uncorrelated obligors to an individual one. However, for larger values of  $\lambda$  the influence of the uncorrelated jumps becomes more dominant leading to a less pronounced dependence on the correlation strength  $c$ . The unexpected loss UL increases both with the jump intensity  $\lambda$  and with the correlation  $c$ . As the correlation changes from 0 to 1, the dependence of UL on the jump intensity changes from a square-root-type-of behavior to a linear one. The expected loss EL (not shown) grows linearly with the jump intensity and is independent of the correlation strength and the portfolio size.

### F. Correlated jumps

In the previous section, we considered a correlated diffusion process with uncorrelated jumps. Now we study the case where also the jumps are correlated, i.e. a jump can occur both in the branch specific time series  $\eta_{b(k)}(t)$  and in the branch independent time series  $\varepsilon_k(t)$ . The jump sizes are scaled with the correlation coefficient ac-

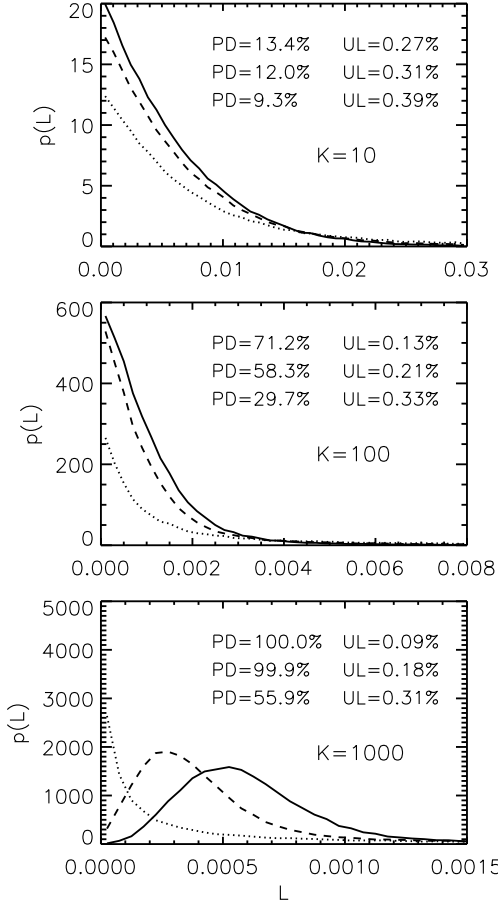


FIG. 18: Loss distributions for portfolios with different branch size. The top left plot shows the structure of the correlation matrix, only the companies within the grey block are in the branch. The other three plots show the loss distributions for three different portfolio sizes  $K = 10, 100, 1000$ , respectively. The branch sizes are (in percent of  $K$ )  $\kappa_1 = 30\%$  (solid lines),  $\kappa_1 = 60\%$  (dashed lines) and  $\kappa_1 = 100\%$  (dotted lines). The expected loss is 0.076% for all three branch sizes. The insets show, for every portfolio size, the portfolio default probability PD and the unexpected loss UL from top to bottom for  $\kappa_1 = 30\%, 60\%, 100\%$ .

cording to Eq. (5). We consider a correlation structure with five branches of size  $K/5$ . In Figs. 23 and 24 the portfolio default probability PD and the unexpected loss UL are displayed as functions of the jump intensity  $\lambda$  and the branch correlation  $c$ . As the correlation changes from 0 to 1, both PD and UL show a transition from  $K$  uncorrelated obligors to the behavior of the five branches. For higher jump intensities, this transition can be non-monotonous — for  $K = 10$  we observe a maximum in PD at  $c \approx 0.3$  and a minimum in UL at  $c \approx 0.35$ . It is important to note that the unexpected loss UL increases tremendously with the correlation coefficient. The expected loss EL (not shown) grows linearly with the jump intensity and is independent of the portfolio size. For fixed jump intensity it shows a minimum at  $c = 0.5$  due

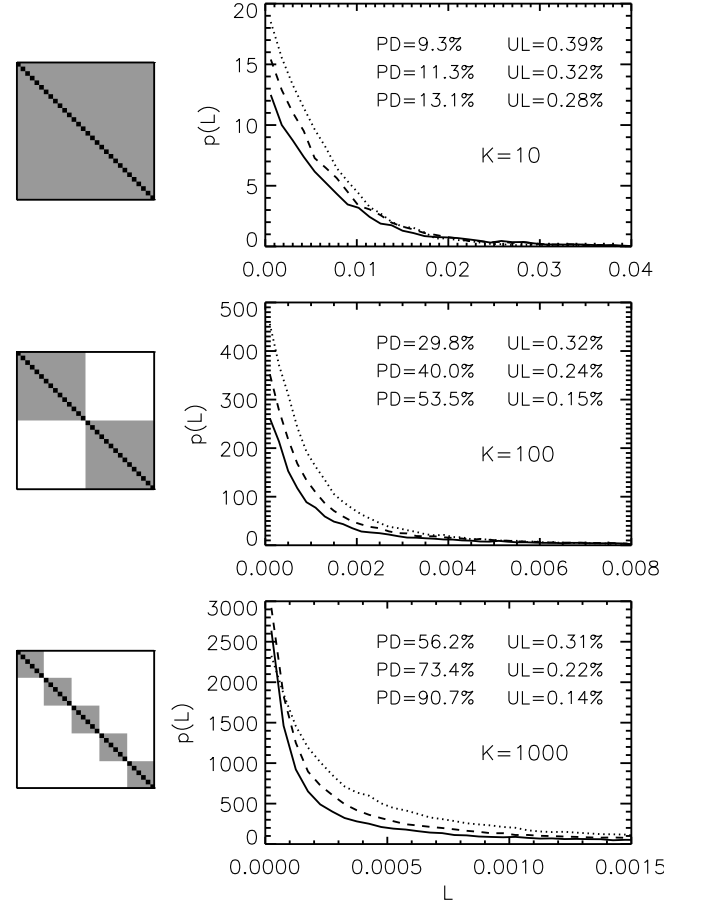


FIG. 19: Loss distributions for portfolios with different number  $B$  of branches. The left column shows the structure of the correlation matrices, labeled C1, C2, C3, respectively. The right column shows the loss distributions for three different portfolio sizes  $K = 10, 100, 1000$  for C1 (solid lines), C2 (dashed lines) and C3 (dotted lines). The branch correlation is  $c = C_b = 0.5$ . The default probability is 1.49%. The insets show, for every portfolio size, the expected loss EL and the unexpected loss UL from top to bottom for C1, C2, C3.

to the scaling of jump sizes according to Eq. (5).

In Figure 25 we show how the loss distributions are affected by introducing correlations. We compare three cases: uncorrelated jump diffusion, correlated diffusion with uncorrelated jumps and fully correlated jump diffusion, as discussed above. As correlation structure we choose again five branches of size  $K/5$ , and the correlation coefficient for each branch is set to  $c = 0.5$ . In the case of correlated jumps, we rescaled the jump intensity and jump sizes, so that they match the uncorrelated case. The correlations in the diffusion already lead to fatter tails; introducing correlations between the jumps enhances this effect. For the case of only five branches, it is most visible in smaller and medium sized portfolios. Figure 26 shows the loss distribution for  $K = 1000$  and a correlation structure with 50 equally sized branches.



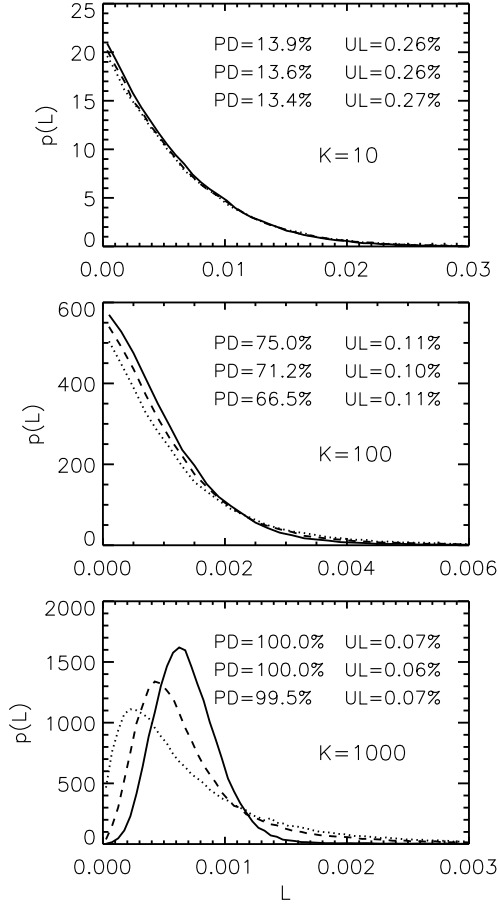


FIG. 20: Loss distributions for portfolios where the product of the branch size and the branch correlation is constant. The top left plot shows the structure of the correlation matrix. The other three plots show the loss distributions for three different portfolio sizes  $K = 10, 100, 1000$ , respectively. The branch sizes are (in percent)  $\kappa_1 = 10\%$  (solid lines),  $\kappa_1 = 50\%$  (dashed lines) and  $\kappa_1 = 90\%$  (dotted lines). The expected loss is 0.076% for all three branch sizes. The insets show, for every portfolio size, the portfolio default probability PD and the unexpected loss UL from top to bottom for  $\kappa_1 = 10\%, 50\%, 90\%$ .

The correlation of the diffusion terms leads to an only slightly fatter tail of the distribution, while the correlation of the jumps has a much more pronounced effect on the tail behavior.

### G. Drill down risk

Finally, we consider how different indicators behave when removing one company from a portfolio of initial size  $K$ . We start with a portfolio which is composed in a rather realistic way. It consists of a large portion of low risk bonds, but also contains a portion of more risky ones. The portfolio was divided into five different categories

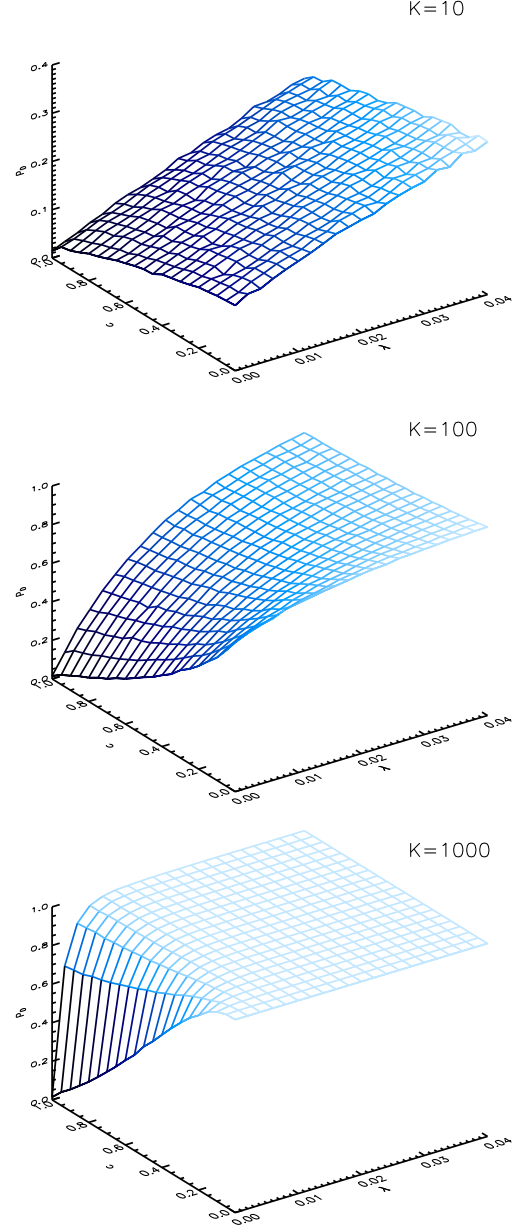


FIG. 21: Portfolio default probability PD as a function of the jump intensity  $\lambda$  and the correlation parameter  $c$  for different portfolio sizes  $K = 10, 100, 1000$ , respectively.

$\zeta = 1, 2, \dots, 5$ . Each category has its own setup of the initial values  $V_0$  and face values  $F$ . All companies within a single branch are identical. The portfolio composition is summarized in Tab. (II). The fraction of the  $K$  companies that belongs to a certain category is  $\alpha$  and the fraction of the total amount of money invested in that category is denoted  $\gamma$ .

Next it has to be decided which company should be removed from the portfolio. A ranking system is established with respect to the product of the default proba-

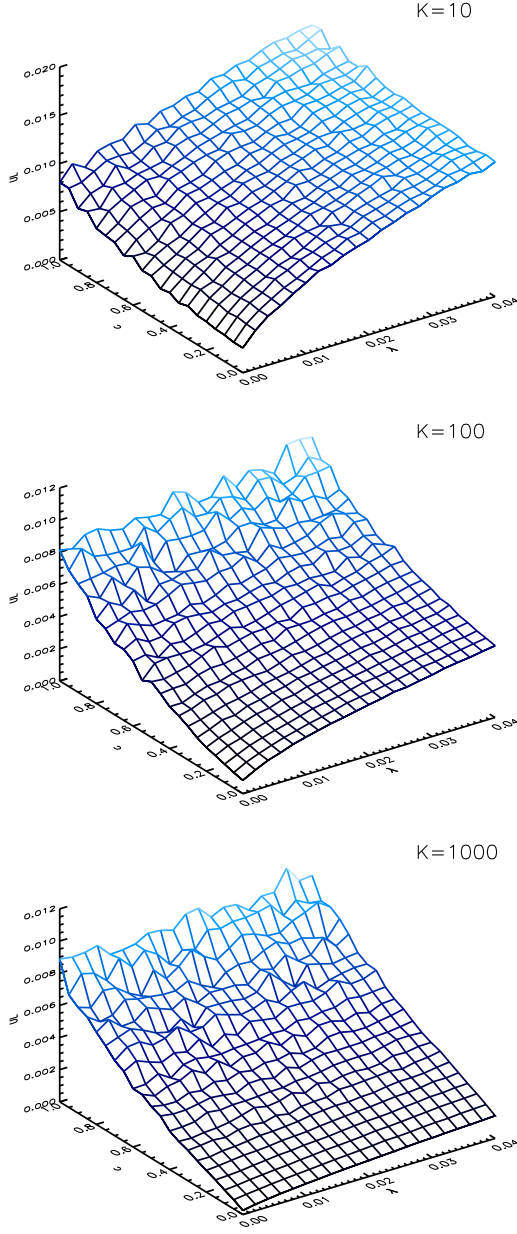


FIG. 22: Unexpected loss  $UL$  as a function of the jump intensity  $\lambda$  and the correlation parameter  $c$  for different portfolio sizes  $K = 1, 10, 100, 1000$ , respectively.

bility and the mean loss

$$R_k = P_{Dk} \mu_k \quad (32)$$

for company  $k$ . The company with the highest value of  $R_k$  is considered to be the worst, and is the one which is removed. By using this ranking system one of the companies in category five will be removed, since they have the highest default probability and expected loss in the entire portfolio.

The different indicators can be seen in Fig. (27), as a function of  $K$ . Naturally, smaller portfolios are more

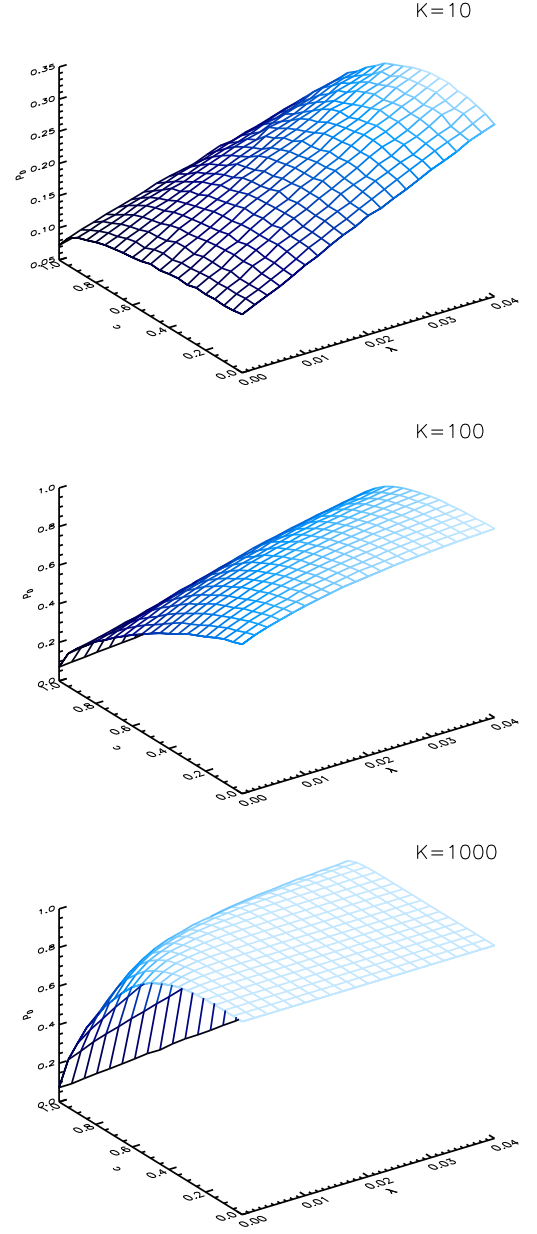


FIG. 23: Portfolio default probability  $PD$  as a function of the jump intensity  $\lambda$  and the correlation parameter  $c$  for different portfolio sizes  $K = 10, 100, 1000$ , respectively.

sensitive to the pruning procedure. For example, when going from  $K = 50$  to  $K = 49$ , the  $EL$  is reduced by about 16% and the  $UL$  is reduced by an enormous 18%! The same comparison when going from  $K = 1000$  to  $K = 999$  is less dramatic but none the less quite significant. In this case the  $EL$  is reduced by 0.75% and the  $UL$  by 0.88%.

The shape of the loss distribution is also affected slightly when removing only one single company. Both the skewness and kurtosis are *increased*, when going from  $K$  to  $K - 1$  companies. On the other hand, both the

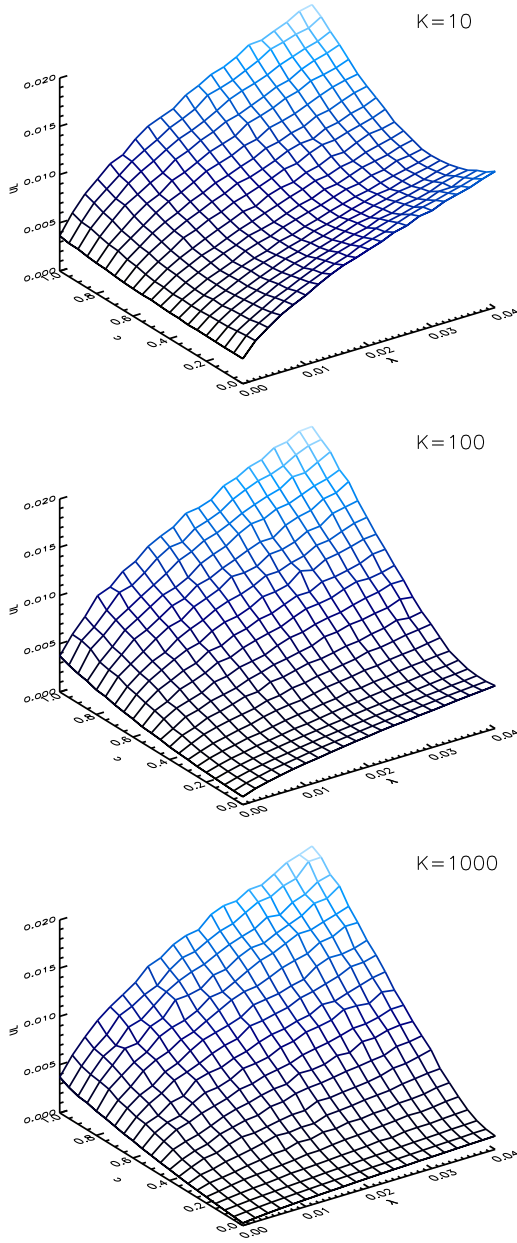


FIG. 24: Unexpected loss  $UL$  as a function of the jump intensity  $\lambda$  and the correlation parameter  $c$  for different portfolio sizes  $K = 1, 10, 100, 1000$ , respectively.

99.9:th percentile  $\alpha_{0.999}$  and the economical capital  $EC$  are decreased.

### 1. Drill down risk in the presence of correlations

How are the moments, and other indicators changed when there are correlations involved? In this section the portfolio, composed by the rule set in Tab. II, is divided into ten different branches. Each branch is correlated with correlation strength one half ( $C_b = 0.5$ ). Note that

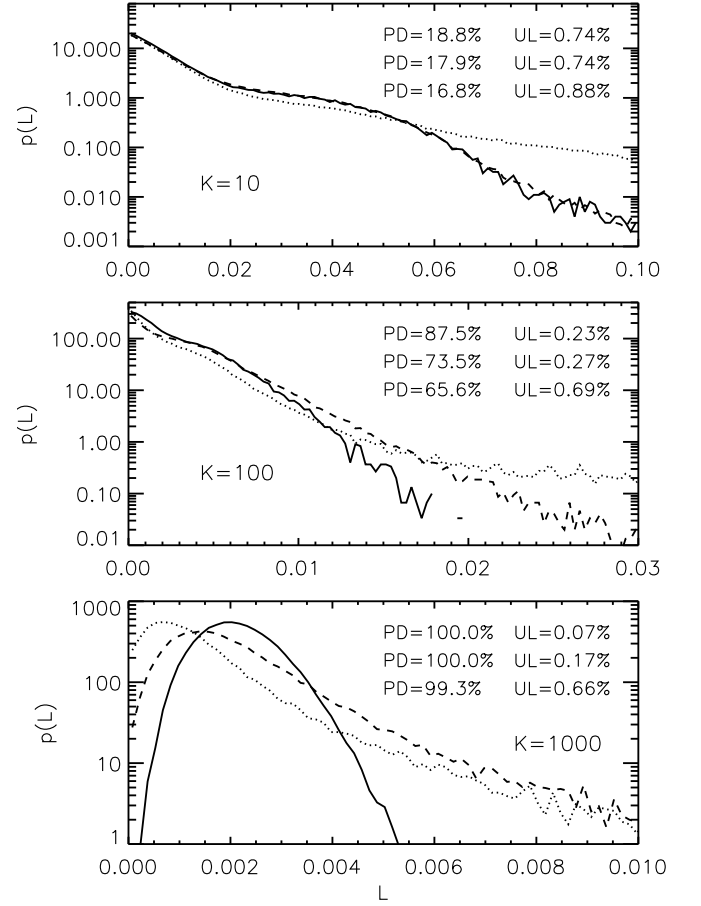


FIG. 25: Loss distributions for uncorrelated jump diffusion (solid lines), correlated diffusion with uncorrelated jumps (dashed lines) and correlated jump diffusion (dotted lines) for three different portfolio sizes  $K = 10, 100, 1000$ , respectively. The insets show, for every portfolio size, the portfolio default probability PD and the unexpected loss UL from top to bottom for the uncorrelated case, correlated diffusion with jumps and correlated jump diffusion.

$\zeta$	$V_0$	$F$	$\alpha$	$F/V_0$	$\gamma$
1	75	50	0.5	0.67	0.355
2	100	75	0.3	0.75	0.319
3	125	100	0.1	0.80	0.142
4	150	125	0.08	0.83	0.142
5	175	150	0.02	0.86	0.042

TABLE II: Portfolio distribution, where  $F$  is the face value and  $V_0$  is the initial value of the company. The fraction of the  $K$  companies that belongs to a certain category is  $\alpha$  and the fraction of the total amount of money invested in that category is denoted  $\gamma$ .

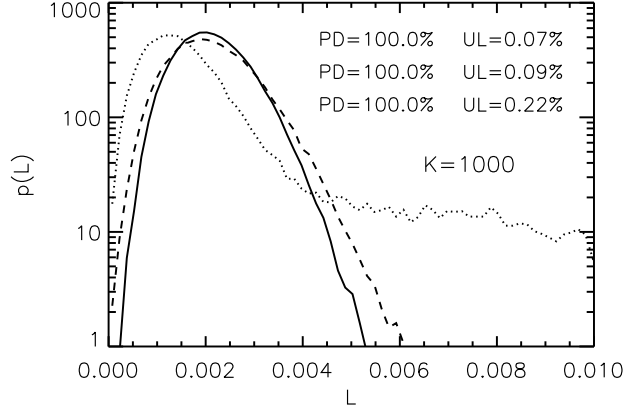


FIG. 26: Loss distributions for uncorrelated jump diffusion (solid lines), correlated diffusion with uncorrelated jumps (dashed lines) and correlated jump diffusion (dotted lines) for portfolio size  $K = 1000$  and 50 branches. The insets show the portfolio default probability PD and the unexpected loss UL from top to bottom for the uncorrelated case, correlated diffusion with jumps and correlated jump diffusion.

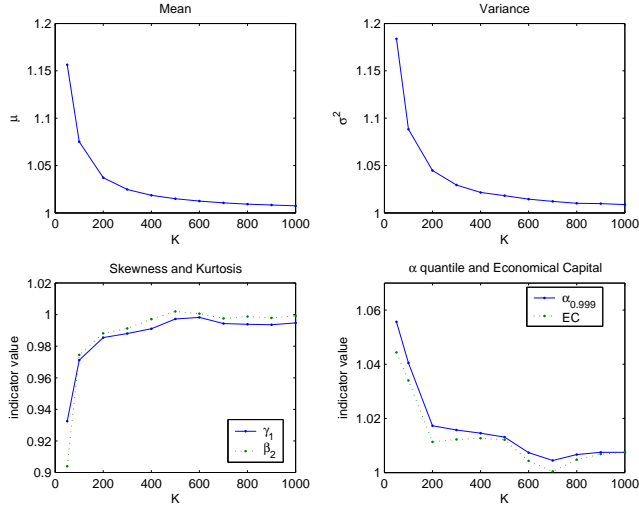


FIG. 27: The ratio between the different indicators as a function of the portfolio size  $K$ . The indicators are calculated from the loss distribution using a portfolio generated by the rule set in Tab. (II). The ratios are calculated as  $x^{(K)}/x^{(K-1)}$ , where  $x$  is the current indicator in focus.

a branch is not equivalent to a category. The concept of categories is developed as a tool to generate portfolios. However, companies which belong to the same branch are generally from different categories.

The companies are assigned to the branches randomly for each iteration. This assures that, for example, two of the high risk companies in the portfolio will not be correlated with each other every time the simulation is run. In Fig. 28 the indicators are plotted as a function

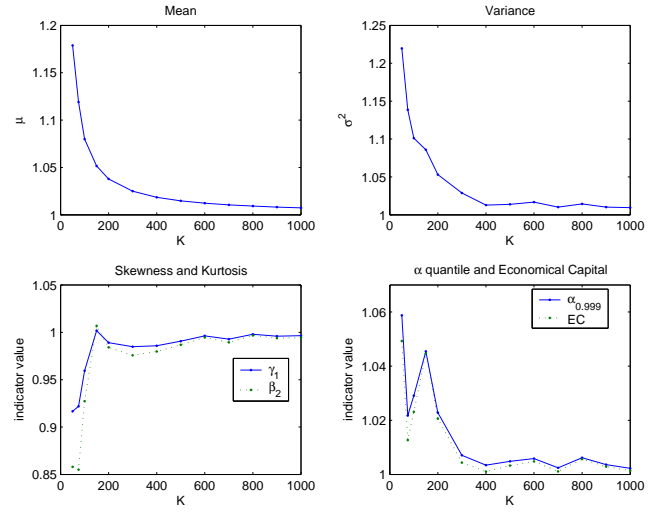


FIG. 28: The ratio between the different indicators as a function of the portfolio size  $K$ . The companies were divided into  $B = 10$  branches and with correlation strength  $C = 0.5$ . The indicators are calculated from the loss distribution using a portfolio generated by the rule set in Tab. II. The ratios are calculated as  $x^{(K)}/x^{(K-1)}$ , where  $x$  is the current indicator in focus.

of the portfolio size  $K$ . For a portfolio of size  $K = 50$  the  $EL$  is improved by about 18%, and the  $UL$  by 22%. For a large portfolio with  $K = 1000$  companies one finds the improvement in  $EL$  to be 0.74% and about 0.72% for the  $UL$ . The skewness and kurtosis decrease slightly, and the  $\alpha_{0.999}$ -quantile and the economical capital  $EC$  are both improved.

## 2. Drill down risk in the presence of jumps

Finally, we examine how the jump term  $J(t)$  alters the pruning of a portfolio. To make this effect as clear as possible the correlations between the bonds are turned off. The jump probability is set to  $\lambda = 0.01$ , along with the parameters  $\mu_J = -0.4$  and  $\sigma_J = 0.3$ .

In this simulation, all bonds have the same parameters for the jump term. The portfolio is again generated by the rule set in Tab. II. In Figure 29 the various indicators are shown as a function of the portfolio size  $K$ .

The benefit of removing the worst company from the portfolio is quite impressive. In these settings the  $EL$  is reduced by 10%, when having a portfolio with original size  $K = 50$ . The  $UL$  is improved by 9% for the same portfolio size. Even though these improvements are large, they are still somewhat lower than in the case without jumps. The jump term tends to smear out the differences between the companies in the portfolio, making them all behave worse. This means that the company which is removed doesn't stand out as much as it otherwise would. This fact is reflected in the ratio between the indicators seen in Fig. 29.

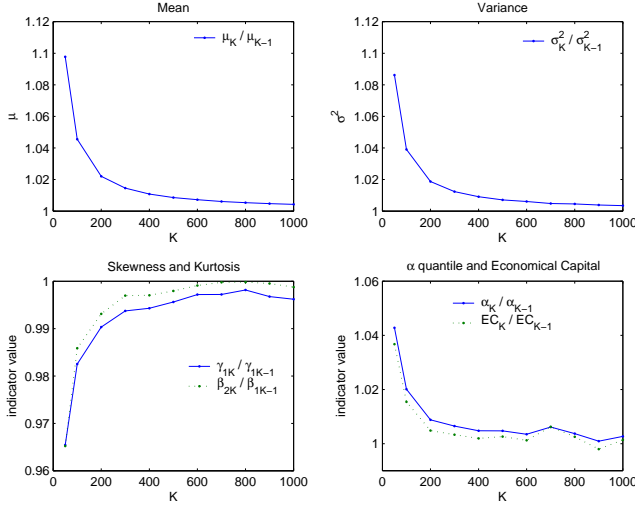


FIG. 29: The ratio between the different indicators as a function of the portfolio size  $K$ , when the jump term  $J(t)$  is included. The parameters for the jump term are  $\sigma_J = 0.3$ ,  $\mu_J = -0.4$  and  $\lambda = 0.01$ . The portfolio was generated by the rule set in Tab. II. The ratios are calculated as  $x^{(K)} / x^{(K-1)}$ , where  $x$  is the current indicator in focus.

As in the previous studies the skewness and kurtosis will increase when removing one company, whereas the  $\alpha_{0.999}$ -quantile and the  $EC$  will improve by as much as four percent for portfolios of initial size  $K = 50$ .

## VI. SUMMARY AND CONCLUSIONS

The microscopic and dynamical character make structural credit risk models well suited for a variety of different applications in physics and complex systems. We formulated a structural model for credit risk which includes jumps in the stochastic processes for the asset prices and correlations between them. As a first step, we solved a simplified version of the model, i.e. without jumps and correlations, analytically and obtained an asymptotic approximation. Thereafter, we numerically evaluated loss distributions and the corresponding expected loss  $EL$  and the unexpected loss  $UL$ . To this end, we performed detailed Monte Carlo simulations for the full model. For theoretical and practical purposes, the asymmetric and leptokurtic character of the loss distribution is highly important. Hence, we carefully investigated how the shape of the loss distribution depends on the various model parameters. First, we illustrated that a large portfolio is less risky than a small one, in accordance to a basic concept of investment theory known as diversification. Second, we demonstrated the influence of growing maturity and the interplay between drift and volatility.

Having presented the basic features of our model, we turned to more advanced issues which are not only of theoretical interest, but might also be of direct relevance

for practitioners. The portion of the company's assets which is financed by loans, the leverage, affects the default probability and the losses rather dramatically. A high leverage induces a high default probability and large losses. Since the default probability strongly depends on the leverage, the sensitivity of the loss distribution to the leverage considerably grows with the portfolio size.

Taking the jumps into account, we demonstrated, first, that an increase of the jump intensity, the jump size mean as well as the jump size standard deviation induced larger losses and higher default probabilities. Second, we showed that the impact of the jump on the loss distribution does not depend on the portfolio size in the same way as, for example, on the drift and the volatility.

Correlations heavily influence the loss distribution and the default probability. Although the expected loss is independent of the branch correlation, the correlations do affect the features of the loss distribution. We carefully illustrated how the correlations hamper a convergence to a symmetric Gaussian-type-of shape and showed that the kurtosis excess develops a maximum. Moreover, the impact of the correlation structure depends significantly on the size of the correlations. Strong correlations make a branch act like a single company. We also showed that a small, highly correlated branch gives essentially the same model outcome as a large branch with a modest correlation.

There is a subtle interplay between jumps and correlations. The uncorrelated jumps can partly neutralize the correlations. Economically, it is also meaningful to include correlations between the jumps themselves. We have demonstrated that correlated jumps have a pronounced effect on the loss distribution, leading to extremely fat tails.

We investigated how the moments of the loss distribution will be influenced when adding a new company to a given portfolio. It was shown that it is possible to express the moments of the loss distribution for a portfolio that consists of  $K$  companies in terms of the moments of the  $K - 1$  sized portfolio. In addition, we studied numerically how different indicators, such as the expected loss, unexpected loss, skewness, kurtosis, economical capital and the  $\alpha_{0.999}$ -quantile, behave when removing one company from a given portfolio. We examined three portfolio setups, one with and one without correlations, and the third one including jumps. For all three setups it was found that both the  $EL$  and  $UL$  was decreased whereas the skewness and kurtosis was increased. Furthermore, the  $\alpha_{0.999}$ -quantile and the economical capital decreased. These effects were more pronounced for smaller portfolios.

When comparing the ratios of the different indicators used, it was found that, in general, correlations *increase* the indicator ratios, whereas jumps tend to *decrease* the indicator ratios.

### Acknowledgments

We thank P. Jochumzen and A. Müller-Groeling for fruitful discussions and helpful comments. We acknowledge financial support from Det Svenska Vetenskapsrådet. RS is grateful for support from Deutsche Forschungsgemeinschaft under grant no. SCHA 1462/1-1.

### APPENDIX A: LOSS DISTRIBUTION FOR A HOMOGENOUS PORTFOLIO

We express the distribution (17) in terms of its Fourier transform,

$$p(L) = \frac{1}{2\pi} \int_{-\infty}^{+\infty} r(\omega) \exp(-iL\omega) d\omega, \quad (\text{A1})$$

where

$$r(\omega) = \prod_{k=1}^K \int_0^1 dL_k p_k(L_k) \int_{-\infty}^{+\infty} dI_k \tilde{p}_k(I_k) \exp(i\omega L_k I_k / K). \quad (\text{A2})$$

is referred to as characteristic function. If we assume that the face values and the parameters of the geometric Brownian motion are the same for all companies  $k$ , the distributions  $p_k(L_k)$  for the individual losses become the same for all companies. This also holds then for the distributions  $\tilde{p}_k(I_k)$  of the default indicators. Hence, we find

$$\begin{aligned} r(\omega) &= \prod_{k=1}^K \int_0^1 dL_k p_k(L_k) ((1 - P_D) + P_D \exp(i\omega L_k / K)) \\ &= \left( \int_0^1 dL_k p_k(L_k) ((1 - P_D) + P_D \exp(i\omega L_k / K)) \right)^K \\ &= \exp(K \ln((1 - P_D) + P_D Q(\omega / K))) \end{aligned} \quad (\text{A3})$$

with

$$Q(\omega / K) = \int_0^1 dL_k p_k(L_k) \exp(i\omega L_k / K). \quad (\text{A4})$$

As we aim at an approximation for large  $K$ , we expand the exponential to obtain an asymptotic series in  $1/K$ .

Up to third order we have

$$Q(\omega / K) = 1 + \frac{i\omega}{K} \langle L_k \rangle - \frac{\omega^2}{2K^2} \langle L_k^2 \rangle - \frac{i\omega^3}{6K^3} \langle L_k^3 \rangle + \mathcal{O}(1/K^4), \quad (\text{A5})$$

where  $\langle L_k^n \rangle$  is the  $n$ -th moment (13) of the distribution  $p_k(L_k)$ . This yields

$$\begin{aligned} &K \ln((1 - P_D) + P_D Q(\omega / K)) \\ &= i\omega P_D \langle L_k \rangle - \frac{\omega^2}{2K} (P_D \langle L_k^2 \rangle - P_D^2 \langle L_k \rangle^2) \\ &\quad - \frac{i\omega^3}{6K^2} (P_D \langle L_k^3 \rangle + 3P_D^2 \langle L_k \rangle \langle L_k^2 \rangle + 2P_D^3 \langle L_k \rangle^3) + \mathcal{O}(1/K^3). \end{aligned} \quad (\text{A6})$$

Collecting everything, we arrive at the expression (19).

### APPENDIX B: LOSS DISTRIBUTION FOR AN INHOMOGENOUS PORTFOLIO

We generalize approximation (19) to the case of an inhomogenous portfolio with varying face values  $F_k$  and individual loss distributions  $p_k(L_k)$ . To this end we write the portfolio loss as

$$L = \frac{\sum_{k=1}^K F_k L_k I_k}{\sum_{k=1}^K F_k} = \sum_{k=1}^K \gamma_k L_k I_k, \quad (\text{B1})$$

where  $\gamma_k = F_k / \sum_{j=1}^K F_j$  is the fraction of money invested in obligor  $k$ . Following App. A, the characteristic function is then

$$r(\omega) = \prod_{k=1}^K \left( (1 - P_{D,k}) + P_{D,k} Q_k(\omega) \right), \quad (\text{B2})$$

with

$$Q_k(\omega) = \int_0^1 dL_k p_k(L_k) \exp(i\omega \gamma_k L_k). \quad (\text{B3})$$

Expanding the exponential in  $Q_k(\omega)$  yields

$$\begin{aligned} Q_k(\omega) &= 1 + i\omega \gamma_k \langle L_k \rangle - \frac{1}{2} \omega^2 \gamma_k^2 \langle L_k^2 \rangle \\ &\quad - \frac{i}{6} \omega^3 \gamma_k^3 \langle L_k^3 \rangle + \mathcal{O}(\gamma_k^4), \end{aligned} \quad (\text{B4})$$

which finally leads to

$$\begin{aligned} p(L) &\approx \frac{1}{2\pi} \int_{-\infty}^{+\infty} d\omega \exp \left( -i\omega \left( L - \sum_{k=1}^K \gamma_k P_{D,k} \langle L_k \rangle \right) \right) \\ &\quad \exp \left( -\frac{\omega^2}{2} \sum_{k=1}^K \gamma_k^2 (P_{D,k} \langle L_k^2 \rangle - P_{D,k}^2 \langle L_k \rangle^2) \right) \end{aligned}$$



$$\exp\left(-\frac{i\omega^3}{6}\sum_{k=1}^K\gamma_k^3(P_{D,k}\langle L_k^3\rangle + 3P_{D,k}^2\langle L_k\rangle\langle L_k^2\rangle + 2P_{D,k}^3\langle L_k^3\rangle)\right) \quad (\text{B5})$$

$$\times \int_{-\infty}^{+\infty} dI_1 \tilde{p}_1(I_1) \cdots \int_{-\infty}^{+\infty} dI_K \tilde{p}_K(I_K)$$

$$\times \int_0^{F_1} d\Gamma_1 p_1(\Gamma_1) \cdots \int_0^{F_K} d\Gamma_K p_K(\Gamma_K).$$

as a generalized approximation for the loss distribution.

### APPENDIX C: DRILL DOWN RISK

We want to express the moments of the loss distribution for a portfolio which consists of  $K$  companies in terms of the moments of a portfolio which consists of  $K - 1$  companies. The loss of an individual company is given by Eq. (25) and the total loss for a portfolio containing  $K$  companies by Eq. (26). To obtain the distribution of the entire portfolio loss, one needs to average over all distributions of the individual losses  $p_k(L_k)$ , and over the indicator distribution  $\tilde{p}_k(I_k)$ . This is done in the following way, c.f. Eq. (17):

$$p^{(K)}(L^{(K)}) = \int_{-\infty}^{+\infty} dI_1 \tilde{p}_1(I_1) \cdots \int_{-\infty}^{+\infty} dI_K \tilde{p}_K(I_K)$$

$$\times \int_0^{F_1} d\Gamma_1 p_1(\Gamma_1) \cdots \int_0^{F_K} d\Gamma_K p_K(\Gamma_K)$$

$$\times \delta\left(L^{(K)} - \frac{\sum_{j=1}^K \Gamma_j I_j}{\sum_{j=1}^K F_j}\right), \quad (\text{C1})$$

where the upper index  $(K)$  indicates that the total number of companies that are averaged over is  $K$ .

The moments of the loss distribution are defined as

$$\langle (L^{(K)})^n \rangle_K = \int_0^1 (L^{(K)})^n p^{(K)}(L^{(K)}) dL^{(K)}, \quad (\text{C2})$$

where  $L^{(K)}$  is the loss for a portfolio containing  $K$  companies,  $p^{(K)}(L^{(K)})$  is the corresponding probability density function and  $n$  is the order of the moment. The sub index  $K$  in the bracket indicates that the distribution for  $K$  companies,  $p^{(K)}$ , is used. Plugging equation (C1) into (C2) we find

$$\langle (L^{(K)})^n \rangle_K = \int_0^1 dL^{(K)} (L^{(K)})^n$$

$$\times \int_{-\infty}^{+\infty} dI_1 \tilde{p}_1(I_1) \cdots \int_{-\infty}^{+\infty} dI_K \tilde{p}_K(I_K)$$

$$\times \int_0^{F_1} d\Gamma_1 p_1(\Gamma_1) \cdots \int_0^{F_K} d\Gamma_K p_K(\Gamma_K)$$

$$\times \delta\left(L^{(K)} - \frac{\sum_{j=1}^K \Gamma_j I_j}{\sum_{j=1}^K F_j}\right). \quad (\text{C3})$$

Integration over  $dL^{(K)}$  yields

$$\langle (L^{(K)})^n \rangle_K = \left( \frac{\sum_{j=1}^K \Gamma_j I_j}{\sum_{j=1}^K F_j} \right)^n \quad (\text{C4})$$

We introduce the sum over all the face values

$$F^{(K)} = \sum_{j=1}^K F_j \quad (\text{C5})$$

and rewrite the sum in Eq. (C4) as

$$\frac{\sum_{j=1}^K \Gamma_j I_j}{F^{(K)}} = \frac{\Gamma_K I_K}{F^{(K)}} + \frac{F^{(K-1)}}{F^{(K)}} \underbrace{\frac{1}{F^{(K-1)}} \sum_{j=1}^{K-1} \Gamma_j I_j}_{\equiv L^{(K-1)}}. \quad (\text{C6})$$

Using the binomial theorem to rewrite the  $n$ :th power sum, we find

$$\langle (L^{(K)})^n \rangle_K = \left( \frac{F^{(K-1)}}{F^{(K)}} \right)^n$$

$$\times \int_{-\infty}^{+\infty} dI_1 \tilde{p}_1(I_1) \cdots \int_{-\infty}^{+\infty} dI_K \tilde{p}_K(I_K)$$

$$\times \int_0^{F_1} d\Gamma_1 p_1(\Gamma_1) \cdots \int_0^{F_2} d\Gamma_K p_K(\Gamma_K)$$

$$\times \sum_{\nu=0}^n \binom{n}{\nu} \left( \frac{1}{F^{(K-1)}} \sum_{j=1}^{K-1} \Gamma_j I_j \right)^{n-\nu}$$

$$\times \left( \frac{I_K \Gamma_K}{F^{(K-1)}} \right)^\nu. \quad (\text{C7})$$

This can now be expressed in terms of the moments of the corresponding  $K - 1$  distribution,  $\langle (L^{(K-1)})^n \rangle_{K-1}$ , and the moments of the new distributions,  $\tilde{p}_K(I_K)$  and  $p_K(\Gamma_K)$ , in the following way

$$\langle (L^{(K)})^n \rangle_K = \left( \frac{F^{(K-1)}}{F^{(K)}} \right)^n$$

$$\times \sum_{\nu=0}^n \binom{n}{\nu} \langle (L^{(K-1)})^{n-\nu} \rangle_{K-1}$$

$$\times \frac{\langle I_K^\nu \rangle \langle \Gamma_K^\nu \rangle}{(F^{(K-1)})^\nu}, \quad (\text{C8})$$

where  $\nu$  is an integer. It is important to remember which distribution the bracket notation  $\langle \cdots \rangle$  refers to. The moments of  $I_K$  and  $\Gamma_K$  are taken over the distributions  $\tilde{p}_K(I_K)$  and  $p_K(\Gamma_K)$  respectively, and the moments of  $L^{(K-1)}$  are taken over the distribution  $p^{(K-1)}(L^{(K-1)})$ .

- 
- [1] R. Mantegna and H. Stanley, *An Introduction to Econophysics* (Cambridge University Press, Cambridge, 2000).
  - [2] J. Bouchaud and M. Potters, *Theory of Financial Risks* (Cambridge University Press, Cambridge, 2000).
  - [3] J. Voit, *The Statistical Mechanics of Financial Markets* (Springer, Heidelberg, 2001).
  - [4] R. Axelrod, *The Complexity of Cooperation: Agent-Based Models of Competition and Collaboration* (Princeton University Press, Princeton, 2001).
  - [5] J. Laffont and D. Martimort, *The Theory of Incentives: The Principal-Agent Model* (Princeton University Press, Princeton, 2001).
  - [6] F. Schweitzer, *Modeling Complexity in Economic and Social Systems* (World Scientific, Singapore, 2003).
  - [7] B. Rosenow, R. Weissbach, and F. Altmann, cond-mat/0401329 (2004).
  - [8] R. Kühn and P. Neu, *Physica A* **322**, 650 (2003).
  - [9] P. Neu and R. Kühn, *Physica A* **342**, 639 (2004).
  - [10] J. Molins and E. Vives, in *Modeling cooperative behavior in the social sciences* (Springer, New York, 2005), vol. 779 of *AIP Conference Proceedings*, pp. 156–161, cond-mat/0401378.
  - [11] K. Kitsukawa, S. Mori, and M. Hisakado, *Physica A* **368**, 191 (2006).
  - [12] J. P. L. Hatchett and R. Kühn, *J. Phys. A* **39**, 2231 (2006).
  - [13] C. Zhou, *Journal of Banking and Finance* **25**, 2015 (2001).
  - [14] C. Bluhm, L. Overbeck, and C. Wagner, *An introduction to credit risk modeling* (Chapman & Hall/CRC, 2002).
  - [15] K. Giesecke, *Credit risk modeling and evaluation: an introduction* (Humboldt-Universität zu Berlin, Berlin, 2002).
  - [16] D. Hamilton, ed., *Default & recovery rates of corporate bond issuers* (Moody's Investors Service, New York, 2002).
  - [17] L. Allen and A. Saunders, *Credit risk measurement* (John Wiley & Sons, New York, 2002).
  - [18] M. Bhatia, C. Finger, and G. Gupton, eds., *CreditMetrics<sup>TM</sup> – Technical Document* (J.P. Morgan & Co. Incorporated, New York, 1997).
  - [19] J. Bohn and P. Crosbie, eds., *Modeling default risk* (KMV LLC, San Francisco, 2001).
  - [20] D. Nouy, ed., *Credit risk modelling: current practices and applications* (Basle Committee on Banking Supervision, Basle, 1999).
  - [21] E. Errais, K. Giesecke, and L. Goldberg, *Pricing credit from the top down with affine point processes* (2007), available at SSRN: <http://ssrn.com/abstract=908045>.
  - [22] G. Giese, *Risk* **16**, 73 (2003).
  - [23] M. Crouhy, D. Galai, and R. Mark, *Journal of Banking and Finance* **24**, 59 (2000).
  - [24] F. B. Hanson and J. J. Westman, in *Stochastic theory and control, Proceedings of a Workshop held in Lawrence, Kansas*, edited by B. Pasik-Duncan (Springer, Berlin, 2002), vol. 280 of *Lecture Notes in Control and Information Sciences*, pp. 169–184.
  - [25] C. Zhang and G. Wang, *Insurance: Mathematics and Economics* **32**, 445 (2003).
  - [26] D. Duffie and J. Pan, *Finance and Stochastics* **5**, 155 (2001).
  - [27] B. Hilberink and L. Rogers, *Finance and Stochastics* **6**, 237 (2002).
  - [28] P. J. Schönbucher, *Factor models for portfolio credit risk*, Working Paper, Department of Statistics, Bonn University (200).
  - [29] A. Lucas, P. Klaassen, P. Spreij, and S. Straetmans, *Journal of Banking and Finance* **25**, 1635 (2001).
  - [30] L. Laloux, P. Cizeau, J. Bouchaud, and M. Potters, *Phys. Rev. Lett.* **83**, 1467 (1999).
  - [31] V. Plerou, P. Gopikrishnan, B. Rosenow, L. Amaral, and H. Stanley, *Phys. Rev. Lett.* **83**, 1471 (1999).
  - [32] R. Mantegna, *Eur. Phys. J. B* **11**, 193 (1999).
  - [33] G. Bonanno, N. Vandewalle, and R. Mantegna, *Phys. Rev. E* **62**, 7615(R) (2000).
  - [34] P. Gopikrishnan, B. Rosenow, V. Plerou, L. Amaral, and H. Stanley, *Phys. Rev. E* **64**, 035106(R) (1999).
  - [35] V. Plerou, P. Gopikrishnan, B. Rosenow, L. Amaral, T. Guhr, and H. Stanley, *Phys. Rev. E* **65**, 066126 (2002).
  - [36] L. Giada and M. Marsili, *Phys. Rev. E* **63**, 061101 (2001).
  - [37] L. Giada and M. Marsili, *Physica A* **315**, 650 (2002).
  - [38] T. Guhr and B. Kälber, *J. Phys. B* **36**, 3009 (2003).
  - [39] J. Noh, *Phys. Rev. E* **61**, 5981 (2000).
  - [40] S. Ross, *J. Econ. Theory* **13**, 341 (1976).
  - [41] K. Giesecke, *Journal of Banking and Finance* **28**, 1521 (2004).
  - [42] K. Giesecke and S. Weber, *Journal of Economic Dynamics and Control* **30**, 741 (2006).
  - [43] K. Itô and H. McKean, *Diffusion Processes and their Sample Paths* (Springer, Berlin, 1965).